People's Democratic Republic of Algeria
Ministry of Higher Education and Scientific Research

University M'Hamed BOUGARA – Boumerdes

Institute of Electrical and Electronic Engineering
Department of Power and Control

Final Year Project Report Presented in Partial Fulfilment of
the Requirements for the Degree of

MASTER

In **Electrical and Electronic Engineering**

Option: **Control & Power**

Title:

Optimization and Control of Recycle Compression Systems using PSO Algorithm and PID Controller

Presented by:

- **Achour IDOUGHI**
- **Abdennacer RAMDANI**

Supervisor:

Dr. R. BOUSHAKI

Registration Number:……/2016

DEDICATION

I dedicate this work to my beloved parents for their endless love, support and encouragement;

To my brother Adel and to my two sisters Assia and Fairouz;

To my entire family;

To all my friends who have been there for me, particularly Adel (Baba) and Mustapha (Fafa) and

Finally to everyone I have ever known even for a moment.

Achour IDOUGHI

DEDICATION

To my parents, my grandfather, my brothers, and sisters.

Abdennacer RAMDANI

Acknowledgements

First and Foremost praise is to **ALLAH**, the Almighty, on whom ultimately we depend for sustenance and guidance. We would like to thank Allah for giving us opportunity, determination and strength to do this work.

Then, we would like to express our eternal gratitude to our academic advisor **Dr. Boushaki. R**, for her assistance in guiding us throughout the evaluation of this thesis and for providing us with the facilities that made this work possible.

Our special thanks go to all our friends for their suggestions and ideas throughout the project development.

Finally, we would also like to thank all IGEE teachers for all information and knowledge they provided us throughout our specialization and giving us a chance to appreciate the real meaning of engineering.

ABSTRACT

Centrifugal compressors are the most satisfactory and the widely used in oil and gas companies, however, stable operation of this type of compressors is limited towards low mass flows by the occurrence of an aerodynamic compressor flow instability called the surge. This instability can lead to severe damage of the machine due to large mechanical and thermal loads in the blading, and restrict its performance and efficiency. In this thesis, a method of controlling the stability of a compression system and optimising its efficiency was presented and developed.

Before going through the controlling and the optimising parts of the work, elementary definitions of compressors and surge have been presented. A mathematical model of Greitzer has been used to model our compression system and, using Matlab Simulink, the compressor's model has been built up. As most industries nowadays are using the PID controller to ensure the stability of compression systems, the classical solution (the use of the PID controller) to eliminate surge has been explored. To increase the output discharge pressure of the compressor, thus increase the compressor's efficiency, the particle swarm-optimising algorithm (PSO) is introduced along with the PID controller to the Simulink model.

The PID did stabilise the system in a short time. However, when using it, the compressor's pressure ratio was quite low. This was overcame once using the PSO, where an acceptable pressure ratio was obtained.

Table of contents

TABLE OF CONTENTS

List of figures

LIST OF FIGURES

List of tables

TABLE OF INDICES

	Meaning	Parameter	Meaning
p	The plenum pressure.	T_{ocs}	The stagnation temperature at the rotor outlet.
m	The compressor mass flow.	k_f	The fluid friction constant.
ω	The rotational velocity of the shaft.	T_{01}	The inlet stagnation temperature.
$\psi_c(m,\omega)$	The compressor characteristic.	C_p	The specific heat at constant pressure.
m_t	The throttle flow.	C_v	The specific heat at constant volume.
A_1	The through flow area.	$k = \frac{C_p}{C_v}$	The ratio of specific heats.
L_c	The duct length.	β_{1b}	The inlet blade outlet angle.
V_p	The plenum volume.	ρ_1	The density.
P_{01}	The ambient pressure.	β_{2b}	The rotor blade angle.
a_{01}	The sonic velocity at ambient conditions.	C	The flow coefficient.
J	The inertia of all rotating parts.	A_t	The area of the orifice opening
τ_d	The drive torque.	R	The specific gas constant.
τ_c	The compressor load torque.	$T1$	The temperature at the inlet of the nozzle.
D_{t1}	The diameters at inducer tip	p_1	The pressure at the inlet of the nozzle.
D_{h1}	The diameters at hub casing	p_2	The pressure at the outlet of the nozzle.
D_2	The diameter at the impeller tip	V_1	The downstream volume.
$C_{\theta 1}$	The tangential component of the gas velocity at the inducer exit.	m_f	The mass flow into the downstream volume.
$C_{\theta 2}$	The tangential component of the gas velocity C_2 at the impeller tip.	m_r	The recycle mass flow.
σ	The Stanitz slip factor.	k_r	The gain proportional to the opening of the valve in the recycle loop.
n_{blades}	The number of blades.	Δp_r	The pressure drop across the recycle valve.
Δh_{0s}	Stagnation enthalpy change in the isentropic compression.		
Δh_{0i}	The shock loss.		
Δh_{0f}	The fluid friction loss.		
V_2	The upstream volume.		

TABLE OF INDICES

Parameter	Meaning
$x_{t,i}$	Position of particle i at time‘t’.
$V_{t,i}$	Velocity of particle i at time‘t’.
$V_{t+1,i,j}$	Updated velocity of particle i at dimension j.
$x_{t+1,i,j}$	Updated position of particle i at dimension j.
c_1, c_2	Weighting constants.
r_1, r_2	Random constants between 0 and 1.
Kc, Td, Ti	PID gains.
Ψ_{SL}	Pressure ratio at surge line.
Ψ_{SCL}	Pressure ratio at surge control line.
m_{SC}	Flow at surge line.
m_{SCL}	Flow at surge control line.
d	Difference.
SL	Surge line.
SCL	Surge control line.

Introduction

INTRODUCTION

This work presents results from an investigation on compression system control. The useful range of centrifugal compressor (turbo compressor) is limited by “choking” (stonewall) at high rate flows and by the onset of an instability known as “surge” at low rate flows. Traditionally, this last instability has been avoided by using control systems that prevent the operating point of the compressor from entering the unstable region, which is at the left side of the surge line that is the stability boundary.

This work is motivated by the fact that the compressors are used in a wide variety of applications such as: power generation, industrial gas turbines, pressurisation of gas and fluids in the process industry and transport of fluids in pipelines in one hand; and the fundamental instability problem known as the surge in the other hand, which is facing centrifugal compressors limiting their range of operation at low mass flows. This instability problem has been studied and solution based on surge avoidance is established. This solution is based on keeping the operating point at the right side of the surge line using a surge margin. There is a potential for increasing the efficiency of compressor by allowing the operating point closer to the surge line, which is the case in this project system. The increase in efficiency range is possible with compressor designs where the design is done with such controllers and optimising techniques.

In this project, we will first address the basic operating principles and characteristics of centrifugal compressors. Next, we will develop the classical solution of the surge phenomena using only the classical controller (PID) as a first step. Then, a meta-heuristic technique of optimisation known as Particle Swarm Optimization (PSO) integrated to the system with the PID controller is going to be used as a controlling method with optimisation. Simulation results show promising results the second technique compared to the results obtained using the PID controller alone.

Chapter One

GENERALITIES ON COMPRESSORS AND SURGE PHENOMENON

1.1. Introduction

A compressor can be defined as a machine used to compress compressible fluids, thus increasing their pressure. The fluid can simply air but it can also be natural gas, oxygen, nitrogen, and other industrial gases.

Compressors are widely used in turbocharging of internal combustion engines, air compression in gas turbines used in power plants and for aircraft and marine propulsion. Another main application is pressurization and transportation of gas in pipelines and in the process and chemical industries. **[1]**

Based on the technique used in increasing the pressure of the compressible fluid, compressors can be classified into many types, the following figure gives the exact classification of compressors.

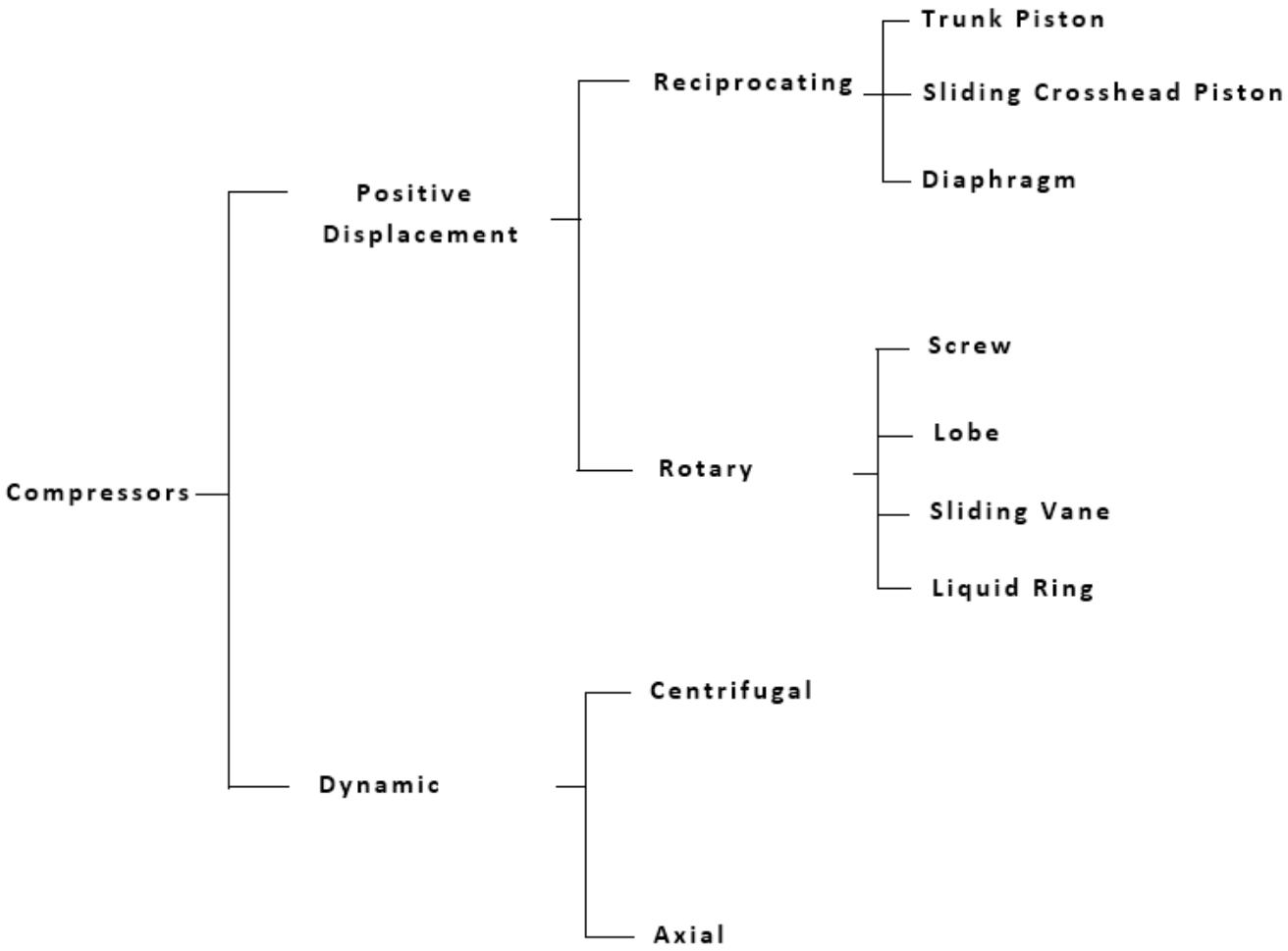

Figure 1.1: Classification Of compressors **[2]**

From **Figure 1.1** two main families of compressors can be distinguished: Positive Displacement compressors and Dynamic compressors.

- Positive displacement compressors increase pressure by reducing the volume occupied by the gas. This type of compressors will not be covered in this final year thesis **[3**].
- Dynamic compressors functions by first accelerating the gas to a high velocity and then hindering its movement so that the gas kinetic energy is converted into static pressure**. [3]**

Dynamic compressors can be further classified into two types of compressors based on the direction of flow through the machine. The two types are:

1. Axial compressors;
2. Centrifugal compressors.

Axial and Centrifugal compressors are also known as turbo compressors or continuous flow compressors. Centrifugal compressors are among the most widely used compressors in industry. Therefore, this thesis will focus on centrifugal compressors. The following figure shows the axial and the centrifugal compressors.

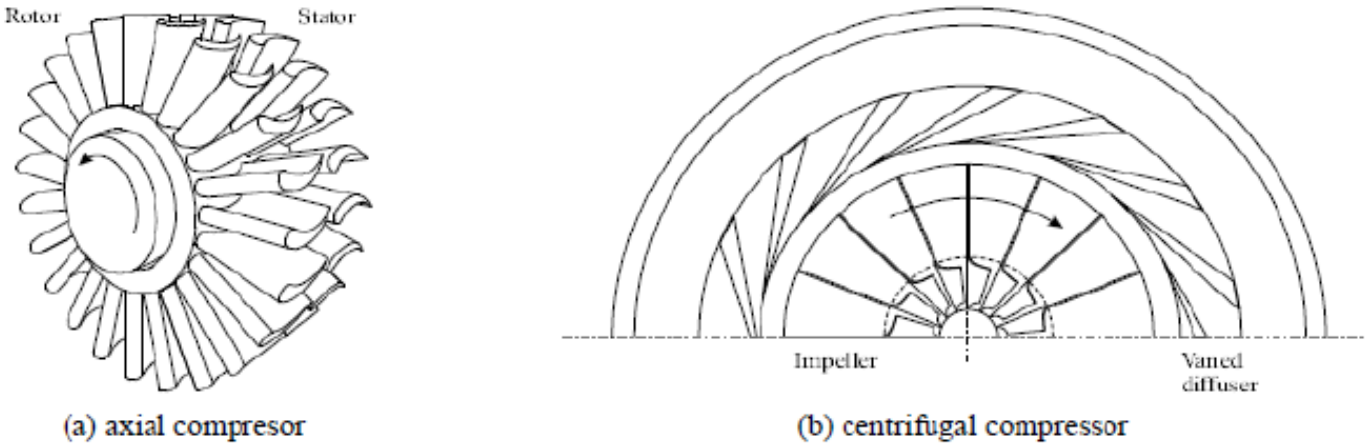

Figure 1.2: Sketch of a Compressor **[4]**

1.2. Centrifugal Compressors

1.2.1. Definition

Centrifugal compressors were first invented in the 19th century by a French professor named Auguste Rateau. **[5]** They are dynamic compressors in which a fluid achieves a pressure rise by adding kinetic energy/velocity to its continuous flow through the impeller. A simple centrifugal compressor has four components: inlet, impeller/rotor, diffuser, and collector. **[6]**

Centrifugal compressor can be Single-stage or Multi-stage. A Single-stage centrifugal compressor has an individual impeller and diffuser pairs while a Multi-stage compressor is a cascade of a single-stage ones. **Figure 1.3** shows the internal view of a five stages centrifugal compressor.

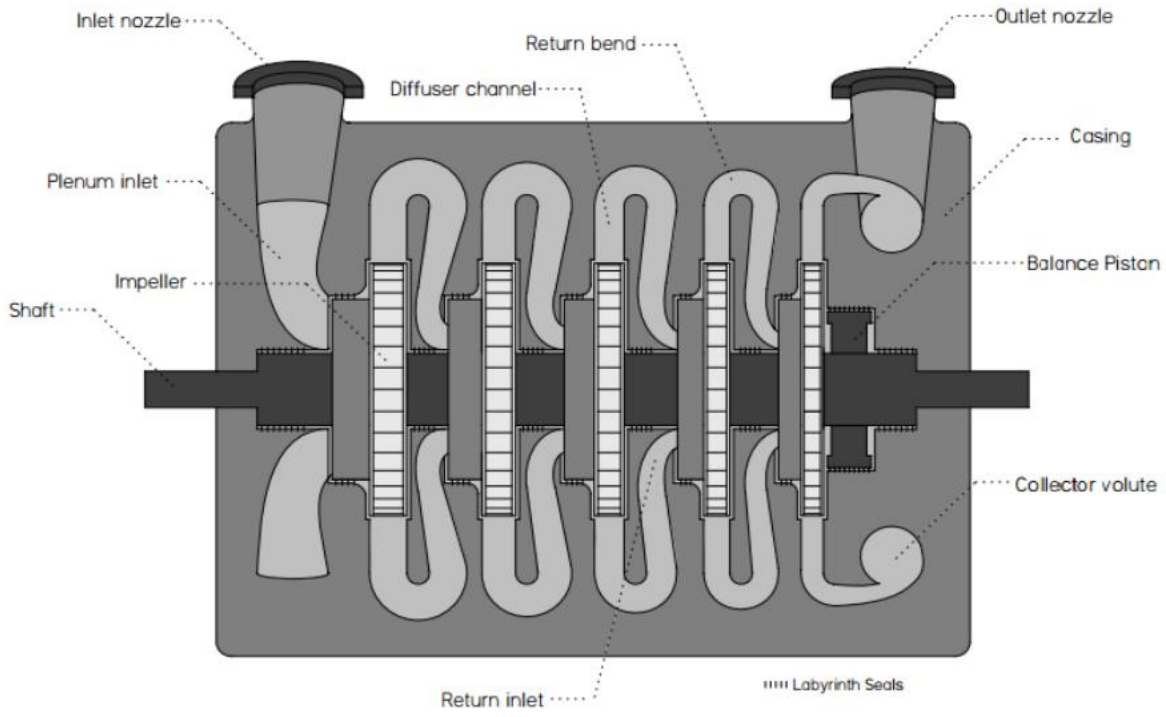

Figure 1.3: Centrifugal Compressor with five stages. **[7]**

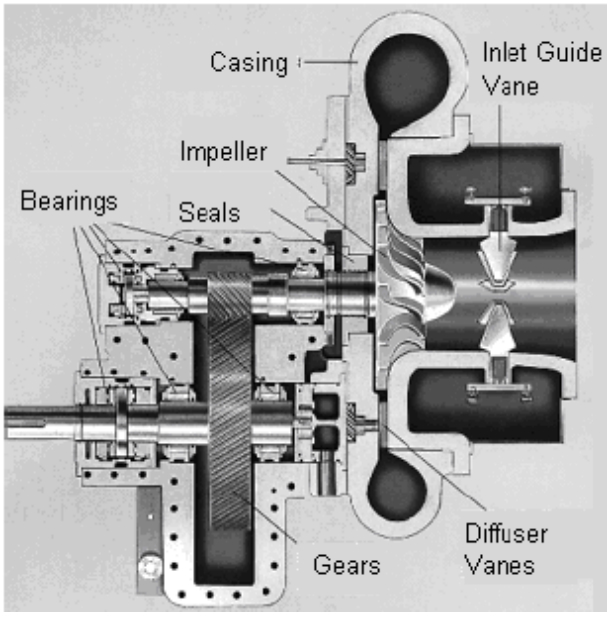

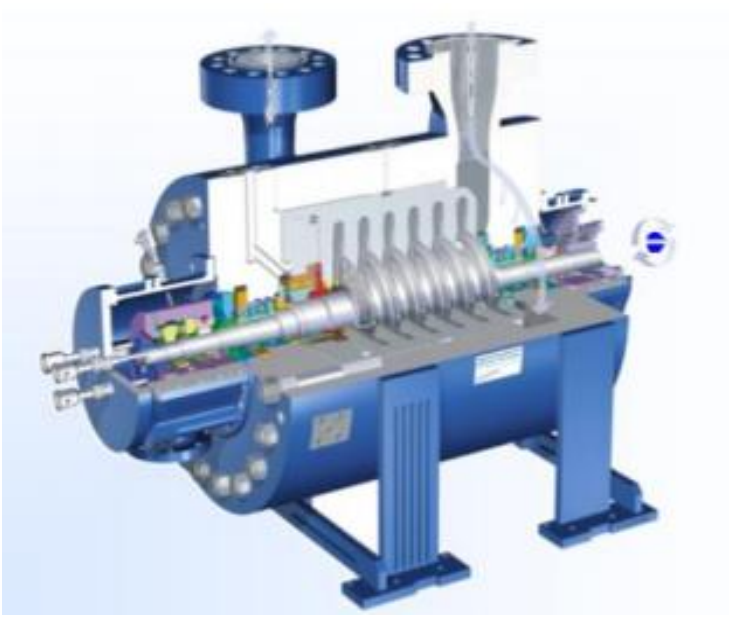

A: Single Stage Centrifugal Compressor **[7]** B: Multi-Stage Centrifugal Compressor **[8]**

Figure 1.4: Real Single and Multi-Stage Centrifugal Compressors.

1.2.2. Principle of operation of a centrifugal compressor

The low pressure fluid enters the compressor through the eye of the impeller, then it enters the flow passages formed by the impeller blades which are connected to the drive shaft. This latter will rotate the impeller at a high speed. As the fluid flows through the passages towards the tip of the rotating impeller, its velocity and static pressure will increase. The fluid will then enter to the diffuser where it is decelerated and as a result the velocity pressure drop is converted into static pressure rise. When the fluid exits the diffuser it is collected by the volute where further conversion of velocity into static pressure takes place due to the divergent shape of the volute. Finally the pressurized fluid leaves the compressor from the volute casing. In some compressors the volute is also used as a diffuser.

In a multistage compressor, different sets of impellers and diffusers are used to increase the pressure of the gas in stages. Labyrinths are installed between the impellers to prevent gas leakage between the stages, each stage has its own casing drain to insure that no liquid is in the compressor before starting.

1.3. Centrifugal Compressors' Performance

The steady performance characteristic of a centrifugal compressor is graphically presented in the form of a family of curves that relate the rotational speed, the pressure rise across the compressor and the mass flow through the compressor (Cumpsty, 1989; De Sa and Maalouf, 1996). That collectively are known as a performance map. **[9] (Figure 1.5)**

The inlet volume flow is plotted along the x -axis and the head or pressure ratio is plotted along the y –axis of the performance map. The pressure ratio is no more than the Absolute outlet pressure divided by the Absolute inlet pressure.

As the flow rate decreases for a given shaft speed, the compressor eventually reaches the critical surge operating point. The Surge point is the lower limit for stable compressor performance. For many given shaft speed values, many surge points are obtained resulting in a line in the map called the "surge line". The higher limit in terms of flow rate on compressor performance curves is set by the stonewall point. Stonewall is another term for choking and occurs when no further increase in flow rate is possible as the fluid reaches the speed of sound at a given shaft speed. Again, for many given shaft

speed values, many stonewall points are obtained resulting in a line in the map called the “stone line” or "choking line". **[3]**

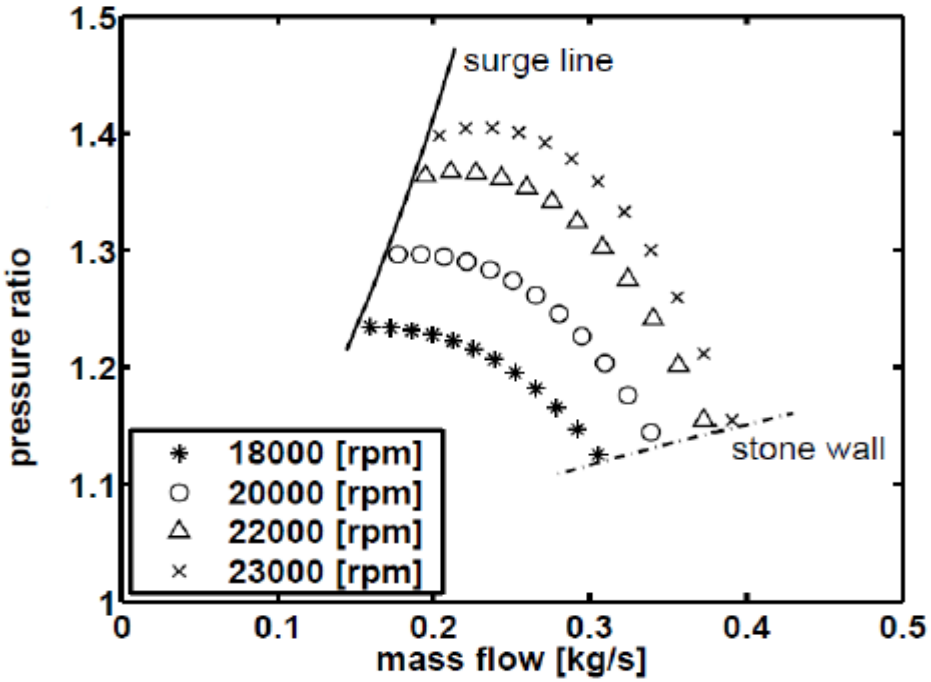

Figure1.5: Compressor's performance map **[4]**

The stability of the compression system is also limited by another phenomenon which is called the chocked (stonewall) phenomenon. In this thesis, the only phenomenon that will be covered is the surge phenomenon.

1.4. Surge phenomenon

1.4.1. Description of surge phenomenon

Surge is defined as the operating point at which the compressor peak head capability and minimum flow limit are reached. When compressor discharge pressure increases because system resistance increases, the operating point will climb on the curve until it reaches the surge line. At this low flow point, the compressor is not able to develop sufficient head.

The compressor loses the ability to maintain the peak head when surge occurs and the entire system becomes unstable. Under normal conditions, the compressor operates to the right of the surge line. However, as fluctuations in flow rate occur, or under start-up / emergency shutdown, the operating point will move towards the surge line because flow is reduced. If conditions are such that the operating point approaches the surge line, the impeller and diffuser begin to operate in stall and flow recirculation

occurs. The flow separation will eventually cause a decrease in the discharge pressure and flow from suction to discharge will resume. This is defined as the surge cycle of the compressor.

Based on the amplitude of mass flow and pressure fluctuations, four categories of surge can be distinguished (De Jager, 1995): mild surge, classic surge, modified surge, and deep surge. **[9]**

1.4.2. Surge cycle

Due to flow reversal, pressure in compressor increases and discharge pressure falls and the compressor regains its normal stable operation (let at point B) delivering the air at higher flow rate at B. But the throttle valve still corresponds to the flow rate at D. Due to this compressor's operating conditions will again return to D through points C and S. And due to lower compressor pressure, the pressure falls further to p_E and the entire phenomenon from point E to B repeats again and again and this cycle E-B-C-S-D-E known as the "**surge cycle". [10]** (**Figure 1.6**)

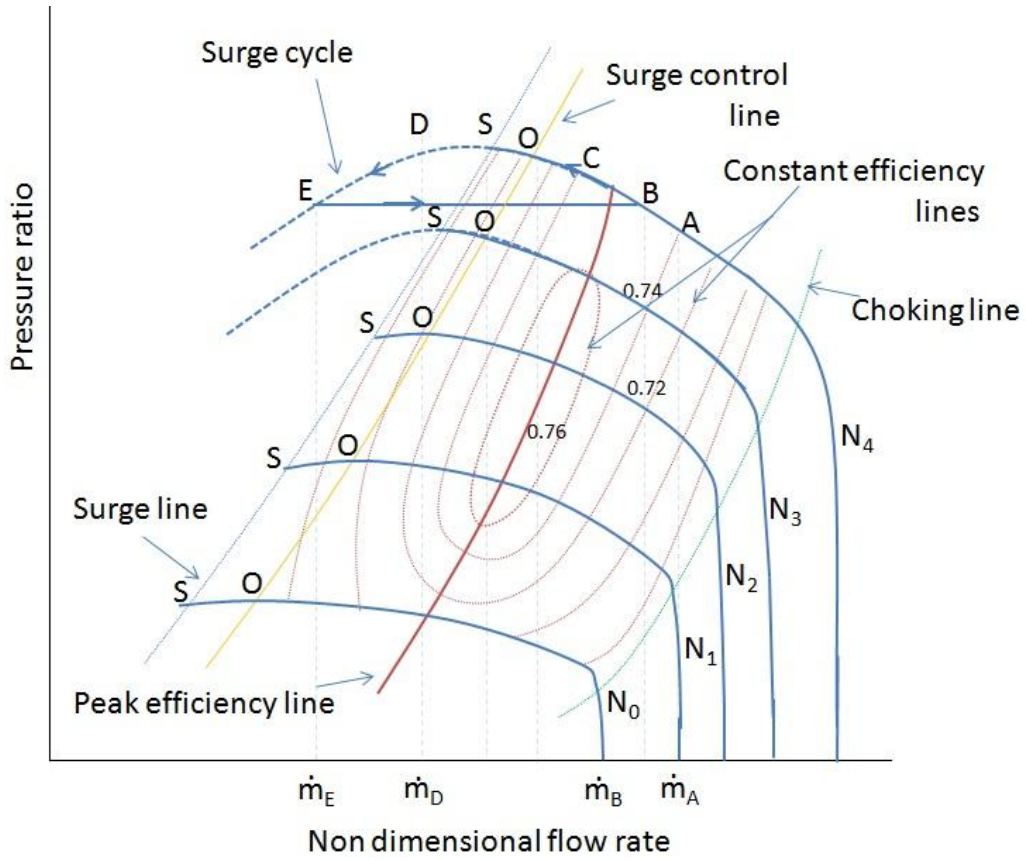

Figure 1.6: Surge cycle [10]

1.5. Surge suppression techniques

It has been seen that surge can lead to failure of the system due to large mechanical loads in the blading. Furthermore, these instabilities restrict the machine's performance and efficiency. As these phenomena are unacceptable, they have to be avoided. Avoidance control and active control are two strategies for compressor's anti-surge control.

1.5.1. Surge avoidance and detection

Stable operation can be guaranteed by operating the compressor at a safe distance from the unstable region. Control systems currently used in industry are based on this control strategy (Botros and Henderson, 1994; CCC, 1997; Gravdahl and Egeland, 1998). In this strategy, a control line is defined at some distance from the surge line, as shown in **Fig. 1.7**. About 10% to the right of the surge line defined by the compressor characteristics. This safety margin is set by (i) sensor and actuator limitations, (ii) uncertainty in the location of the stall line, and (iii) disturbances including load variations, inlet distortions, and combustion noise. If the compressor's operating point tends to cross the control line, it is stuck to the control line by, for example, opening a recycle valve (see, *e.g.*, Botros et al. (1991) or Staroselsky and Nadin (1979)) or decreasing the shaft speed.

However, Surge avoidance limits the performance of the compressor, since the maximal pressure is obtained close to the stall line (Gu et al., 1996). Clearly, the recycle of the compressed fluid is not useful and reduces the overall efficiency. **[9]**

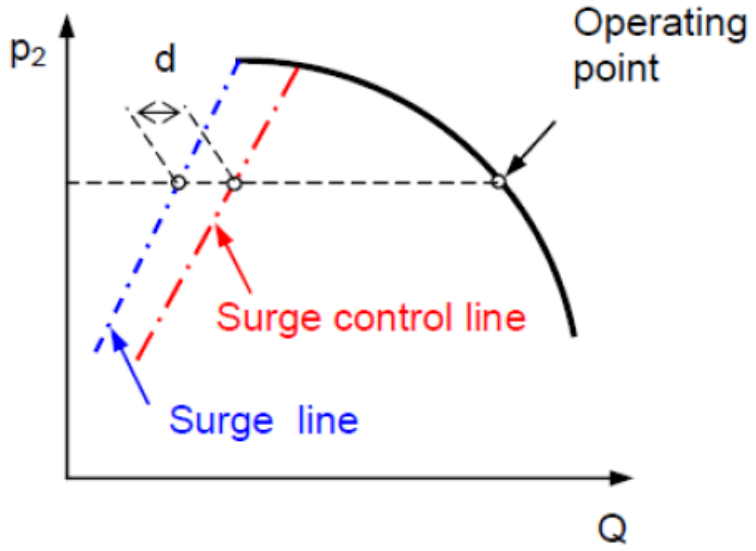

Figure 1.7: Surge line and surge control line **[11]**

1.5.2. Anti-surge Active Control

Another surge solution is to stabilize the surge phenomenon by using an active control system. This method is known as active surge control system (ASCS) and was proposed by Epstein et al. in 1989.

In this approach, controllers are used which stabilize unstable operating points by feeding back perturbations into the flow field. Based on information from sensors, which detect fluid fluctuations, the controller computes the desired perturbations to stabilize the system. These perturbations can be introduced, for instance, by a control valve or a loudspeaker. By feedback control, the compression system dynamics are modified such that the stable operating region is enlarged beyond the "natural" stall line. **[9]**

1.5.3. Difference between surge avoidance and Anti-surge Active Control

It is very important to understand the fundamental difference between prevention control, and avoidance control. Both systems are designed to extend the operating range of the compressor, but the technique and the results are different. Avoidance control is achieved by unloading the compressor thus achieving operation at reduced flow rate, but also at reduced pressure rise. Active, or preventive, control on the other hand aims to damp out the disturbances which cause stall thereby allowing the compressor to operate normally, without an abrupt change in pressure rise, at a flow rate less than is usually possible. **[12]**

1.6. Conclusion

In this chapter, basic definitions and concepts of compressors were presented. A brief definition of a compressor was given at first, then its different uses were discussed. A detailed classification of compressors was also given at the end of the chapter's introduction.

The next point discussed was the centrifugal compressors and their principle of operation. Compressors' performance was covered after that. It is impossible to speak about compressors' performance without dealing with the surge phenomenon which is one of the compressor's instabilities. Thus, a complete explanation of the cyclic surge phenomenon was given.

Since surge is cyclic, a technique for avoiding and suppressing it is needed so that the compressor operates properly. Therefore, it was considered necessary to present the two main techniques of anti-surge control and finally give the difference between them.

Chapter Two

CENTRIFUGAL COMPRESSOR MODELLING

2.1. Introduction

Surge in centrifugal compressors is characterized by large amplitude fluctuations of the pressure and by unsteady, but circumferentially uniform mass flow. This essentially one-dimensional instability results in a limit cycle oscillation in the compressor map. **[13]** These oscillations can cause severe damage to the machine due to vibrations and high thermal loading. Hence anti-surge control systems must be designed to avoid such phenomenon.

But before designing any control system, a simple mathematical model describing its behaviour must be found.

In this chapter, a model describing the behaviour of compression systems in both open loop and closed loop (controlled) configurations is going to be discussed and explored.

2.2. Literature on compression system modelling [14]

Many attempts by different researchers to model the instabilities in both axial and centrifugal compressors have been stated in the literature.

One of the first models reported in the literature was developed by Emmons et al. (1955). However, it is the model proposed by Greitzer (1976a) who developed a nonlinear lumped-parameter model for basic compression systems that had a significant step forward in further studies of surge control. The model was first introduced for axial compressors but it has been used on centrifugal compressors successfully by Hansen et al., (1981) and Pinsley et al., (1991). This was followed by more studies that focused on the analysis and modelling of centrifugal compression system dynamics.

A relevant progress was made by Fink et al. (1992) who included simple rotor dynamics in a Greitzer model to account for the effect of speed variations on system transients.

Based on the work of Moore (1984b), the Moore-Greitzer model was derived in Moore and Greitzer (1986). In developing this model, some of the assumptions made were: Large hub/tip ratio, irrotational and inviscid flow in the inlet duct, incompressible compressor mass flow, short throttle duct, and small pressure rise compared to ambient conditions and constant rotor speed. The model is described by three states. This three state model is capable of describing both surge and rotating stall, the third state being the stall amplitude.

A different modelling approach for centrifugal compressors was followed by Botros et al. (1991) while Badmus et al. (1995a) focused on axial compressors. They developed component models from the principles of mass, momentum, and energy conservation. The modular structure makes them, without serious modifications, suitable for describing surge dynamics of a variety of both axial and centrifugal compression systems.
Botros (1994b) modified his earlier model by including rotor dynamics in order to account for speed variations.

Rotor dynamics were included in the original Moore-Greitzer model by Gravdahl and Egeland (1997). The issue of compressible flow was also addressed by Feulner et al. (1996) who developed a linear compressible flow model for a high speed, multi-stage axial compressor. He used a mixture of 1D and 2D flow descriptions for the blade passages and inter-blade row gaps, respectively. A complete two-dimensional, compressible flow model for a high speed, multi-stage axial compressor was developed by Ishii and Kashiwabara (1996) which is Similar to the Moore-Greitzer model.

Markopoulos et al. (1999) used Fourier series expansions to derive a quantitative model for the unstable dynamics in axial compressors. Although similar to the model of Moore and Greitzer (1986), in this model, finite intake and exit duct lengths were taken into account. A sophisticated two-dimensional, compressible flow model for centrifugal and axial compressors was developed by Spakovszky (2000).

In the Greitzer model, the pressure rise characteristics of the compressor and throttle are described by quasi-static maps that are lumped onto actuator disks. Oliva and Nett (1991) presented a nonlinear dynamic analysis of a reduced Greitzer model in which the pressure rise and throttle characteristics, assumed fixed by Greitzer (1976a), can vary.

Common practice in the literature was and still is to use an approximation of the pressure rise characteristics, for example the cubic polynomial suggested by Greitzer and Moore (1986). Gravdahl and Egeland (1999a) derived an analytical expression for the compressor map, based on compressor geometry and energy considerations.

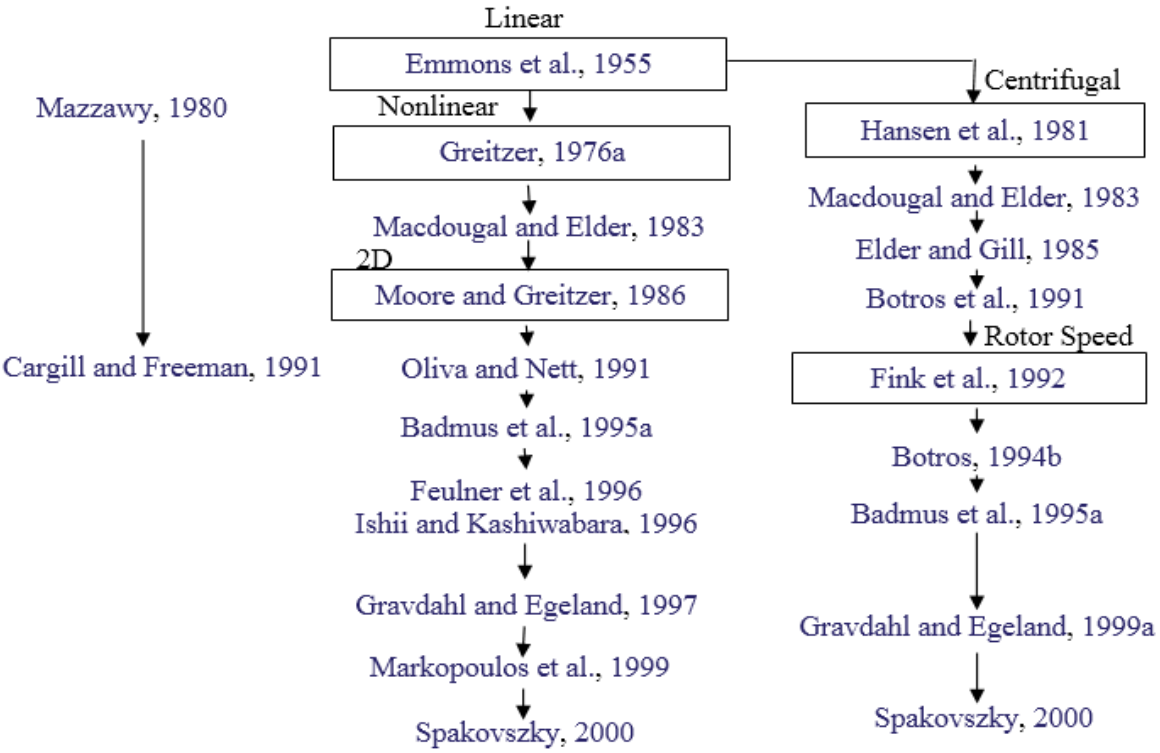

Figure 2.1: Overview of literature on compression system modelling **[14]**

2.3. Compressor Open loop modelling

Greitzer (Greitzer, 1976) considered that the speed of the shaft is constant in his model which is a dynamic compressor model capable of representing the characteristics of surge. Whereas Gravdahl and Egeland did not consider the speed constant; they included the speed state in the compressor dynamics. They used the model of Greitzer which is a basic compression system consisting of a compressor, a plenum volume, a throttle valve and in-between ducting. **[15] (**Figure 2.2**)**

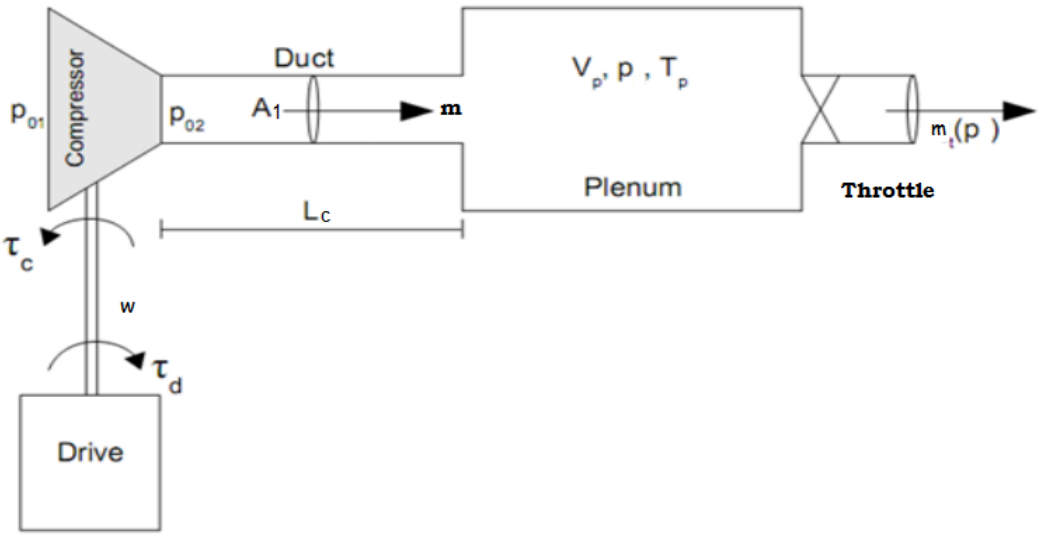

Figure 2.2: The Compressor, Plenum, Throttle System of Open Loop Model **[16]**

Thus, the compressor open loop model is expressed by three state equations including the mass flow, pressure and the rotational speed. The expression for the pressure is found from the mass balance applied on the plenum. Whereas, the expression for the mass flow is found from the momentum balance applied on the duct, and the expression for the shaft dynamics is gotten from the angular momentum relation. **[17]**

The model is written as:

$$\dot{p} = \frac{a_{01}^2}{V_p}(m - m_t) \qquad (\mathbf{2.1})$$

$$\dot{m} = \frac{A_1}{L_c}(\psi_c(m, \omega)p_{01} - p) \qquad (\mathbf{2.2})$$

$$\dot{\omega} = \frac{1}{J}(\tau_d - \tau_c) \qquad (\mathbf{2.3})$$

- p is the plenum pressure;

- m is the compressor mass flow;

- ω is the rotational velocity of the shaft;

- Ψ_c (m, ω) is the compressor characteristic;

- m_t is the throttle flow;

- A_1 is the throughflow area;

- L_c is the duct length;

- V_p is the plenum volume;

- p_{01} is the ambient pressure;

- a_{01} is the sonic velocity at ambient conditions;

- J is the inertia of all rotating parts and

- τ_d and τ_c is the drive torque and compressor load torque, respectively:

Where $$\tau_c = |m| r_2^2 \sigma \omega \qquad (2.4)$$

τ_c Is obtained by applying the energy conservation theory, for turbo-machines, applied torque equals the change in angular momentum of the fluid. **[17]**

$$\tau_c = m(r_2 C_{\theta 2} - r_1 C_{\theta 1}) \qquad (2.5)$$

r_1: is the radius at the inducer exit.
r_2: is the radius at the impeller exit.
$C_{\theta 1}$: is the tangential velocity of the gas at the inducer exit.
$C_{\theta 2}$: is the tangential velocity of the gas at the impeller exit.

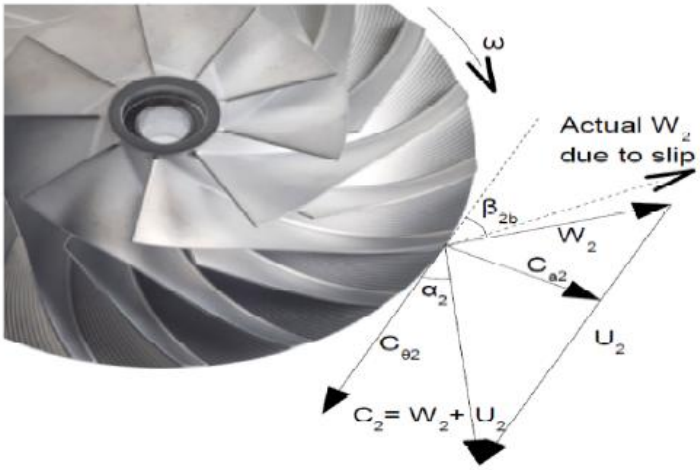

Figure 2.3: Velocity triangle at the impeller exit.

The power delivered to the fluid is:

$$\dot{W}_c = \omega \tau_c = \omega\, m(r_2 C_{\theta 2} - r_1 C_{\theta 1}) = m(U_2 C_{\theta 2} - U_1 C_{\theta 1}) \qquad (2.6)$$

The velocity at the impeller inlet (or at the inducer exit) $C_{\theta 1}$ is considered zero.

For an ideal radially vanned impeller, the whirl or tangential component $C_{\theta 2}$ of the gas velocity leaving the impeller tip should be equal to U_2. However, due to the inertia of the gas

between the impeller blades, the tangential gas velocity tends to be less than U_2. This effect is known as *slip*. The flow is deflected away from the direction of rotation of the impeller, which leaves at an angle smaller than the vane angle. The slip factor is defined as:

$$\sigma \triangleq \frac{C_{\theta 2}}{U_2} \qquad (\mathbf{2.7})$$

It's now easy to compute the compressor's torque τ_c needed in the model described by the previous equations. Using the assumption of no prewhirl and Eq2.7, the compressor torque is:

$$\tau_c = mr_2 C_{\theta 2} = mr_2 \sigma U_2, \qquad m > 0 \qquad (\mathbf{2.8})$$

However, the compressor may enter deep surge, that is reversal of flow, and there is need for an expression for the compressor torque at negative mass flow. **[17]**

$$\tau_c = -mr_2 \sigma U_2, \qquad m < 0 \qquad (\mathbf{2.9})$$

Combing the two equations, we get the following:

$$\tau_c = |m| r_2 \sigma U_2 \qquad (\mathbf{2.10})$$

2.3.1. The Compressor Characteristic [18]

The compressor characteristic is known also as a compressor's performance characteristic. Gravdahl and Egeland in 1999, derived a new expression of the compressor characteristic by modelling the compression process as an isentropic compression from P_{01} to P_{02} by an isobaric entropy increase.

Generally speaking, the compressor characteristic is defined by: $\psi_c(m,\omega) = \frac{P_{02}}{P_{01}}$, P_{02} being the discharge (output) pressure and P_{01} being the ambient pressure.

And using the standard isentropic relations given in [18], the following equation is obtained:

$$\psi_c(m,\omega) = \left(\frac{T_{ocs}}{T_{01}}\right)^{\frac{k}{k-1}} = \left(1 + \frac{\Delta h_{0s}}{C_p T_{01}}\right)^{\frac{k}{k-1}} \qquad (\mathbf{2.11})$$

And after substituting some parameters, the final compressor characteristic is defined as follows:

$$\psi_c(m,\omega) = \left(1 + \frac{\mu r_2^2 \omega^2 - \frac{r_1^2}{2}(\omega - \alpha m)^2 - k_f m^2}{C_p T_{01}}\right)^{\frac{k}{k-1}} \qquad \text{With} \quad k \neq 1 \qquad (\mathbf{2.12})$$

$-r_1$ is the impeller radius, r_2 is the rotor diameter, k_f is the fluid friction constant, T_{01} is the inlet stagnation temperature, $\kappa = \frac{c_p}{c_v}$, c_p is the specific heat at constant pressure, c_v is the specific heat at constant volume. The constant α determines the point of zero incidence loss, which occurs for ω−αm=0.

$$\alpha = \frac{cot\beta_{1b}}{\rho_1 A_1 r_1} = \frac{\omega_{Surge\_line}}{m_{Surge\_line}} \qquad \textbf{(2.13)}$$

Where β_{1b} the inlet blade outlet is angle and ρ_1 is the density.

- Explanation of how Eqs 2.12 is obtained from Eqs 2.11 is explained in **Appendix A.**
- The equation (2.12) can also be considered valid in the unstable area to the left of the surge line.

- There exist another method for modelling the compressor characteristic which is the polynomial approximation which is first used by Moore Greitzer 1986 to replace the old compressor characteristic model. This approximation approximates equation (2.12) with a cubic polynomial whose expression is given as:

$$\psi_c(\phi) = \psi_{c0} + H\left(1 + 1.5\left(\frac{\phi}{w} - 1\right) - 0.5\left(\frac{\phi}{w} - 1\right)^3\right) \qquad \textbf{(2.14)}$$

The parameters of the previous equation are described in the next figure.

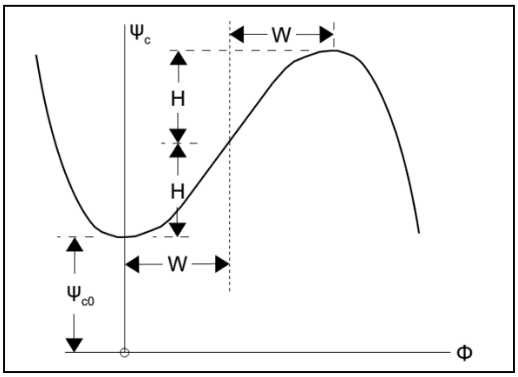

Figure 2.4: Definition of the parameter of the approximated cubic polynomial.

However, Eqs (2.14) is non-dimensional and it represents the pressure rise not the pressure ratio. Moreover, it's only valid for one single speed.

Thus, Egeland and Gravdahl in 2002 approximated each speed line on the compressor's performance map with a third order polynomial of the following form: (m is the mass flow)

$$\Psi_c(m) = c_0 m^3 + c_1 m^2 + c_2 m^1 + c_3 \qquad \textbf{(2.15)}$$

After that, the coefficients were approximated in accordance with the rotational speeds to have a continuous relationship between the pressure ration and the flow as:

$$c_i(\omega) = c_{i0}\omega^3 + c_{i1}\omega^2 + c_{i2}\omega^1 + c_{i3} \quad \textbf{(2.16)}$$

Where ω is the rotational speed, the final equation will be:

$$\Psi_c(m,\omega) = c_0(\omega)m^3 + c_1(\omega)m^2 + c_2(\omega)m^1 + c_3(\omega) \quad \textbf{(2.17)}$$

- Using data of a real compressor from the compressor map of Vortech S-trim superchargers (www.vortechsuperchargers.com), a work has been done by Bjorn Ove Barstad to approximate the nonlinear data with a 3rd order polynomial having the form of Eqs 2.17 using identification. To approximate the parameters of Eqs (2.17), the scientist used MATLAB Polyfit function while plot function is used to plot the approximation.

The data used and the polynomial approximation's representation are shown below:

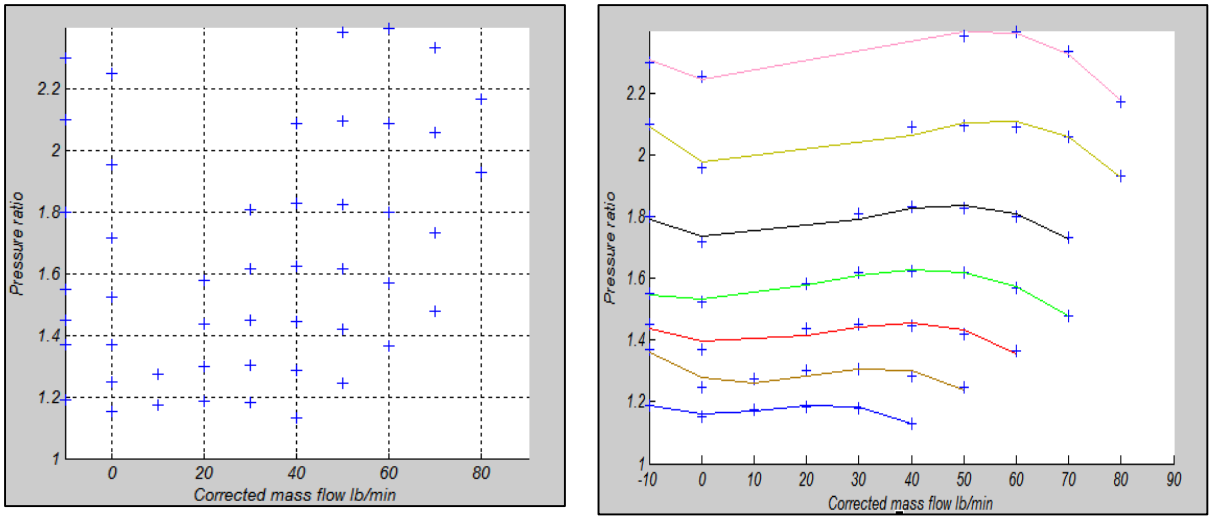

a **b**

Figure 2.5: a) Measurements of a real compressor performance map. **b)** Polynomial approximation of the compressor characteristic.

Remarks

- The model polynomial approximation data is taken from Bjørn Ove Barstad (2010).
- The Matlab files used for the polynomial approximation are given in the **Appendix B.**

2.3.2. The valve model

The flow through the valves used in our model (either throttle valve flow m_t, feed flow valve m_f or recycle valve m_r) can be modelled as flow through a restriction or an orifice. That is: for instant, the flow through the throttle valve is:

$$m_t = CA_2\sqrt{2\rho(p_1 - p_2)} = k_t\sqrt{p_1 - p_2} \qquad (\mathbf{2.18})$$

Where m_t is the mass flow through the opening, C is the flow coefficient, A_2 is the area of the orifice opening, ρ is the density of the fluid, and $\Delta p = p_1 - p_2$ is the pressure drop across the orifice.(p_1 is fluid upstream pressure; p_2 is fluid downstream pressure).

To control the flow through the valve, the orifice area A_t can be adjusted from 0 to 100%. The final model for the flow through the throttle is:

$$m_t = k_{t\%}\sqrt{p_1 - p_2} = k_t\sqrt{\Delta p} \qquad (\mathbf{2.19})$$

To be able to account for the special case $p_1 < p_2$ in Eq2.19, the following modification is done:

$$m_t = sgn(p_1 - p_2)k_{t\%}\sqrt{|p_1 - p_2|} \qquad (\mathbf{2.20})$$

The sgn function is not continuous, but can be approximated as:

$$sgn(x) = \lim_{\varepsilon \to \infty} tanh(\varepsilon x) \qquad (\mathbf{2.21})$$

And the absolute value is approximated by:

$$|x| = x.sgn(x) = x.\lim_{\varepsilon \to \infty} tanh(\varepsilon x) \qquad \mathbf{(2.22)}$$

Thus the flow rate through the throttle valve is given as:

$$m_t = tanh(\varepsilon(p_1 - p_2))k_{t\%}\sqrt{(p_1 - p_2)tanh(\varepsilon(p_1 - p_2))}$$

2.3.3. Model simulation

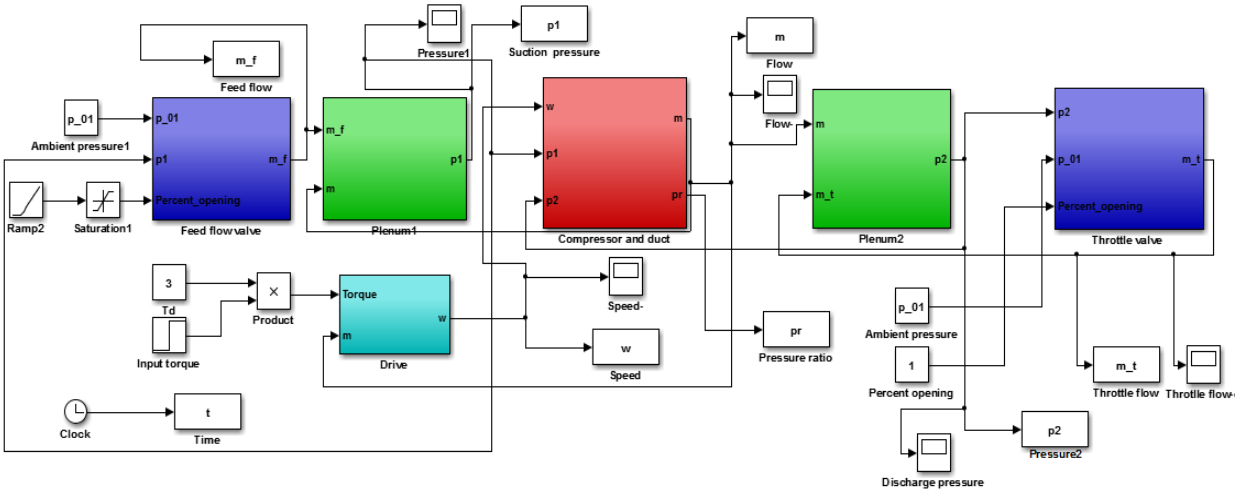

Figure 2.6: Simulink Circuit for the Gravdahl and Egeland Model in Open Loop

The following graphs are obtained after running the previous Simulink file:

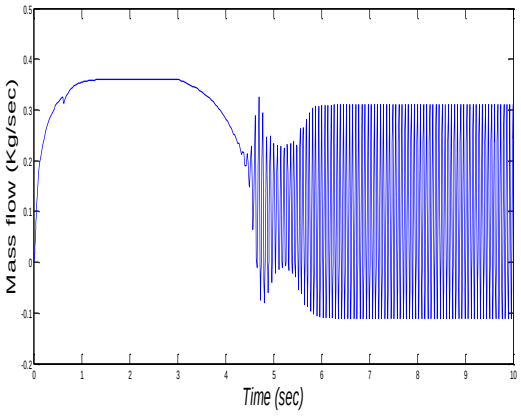

A. Mass flow

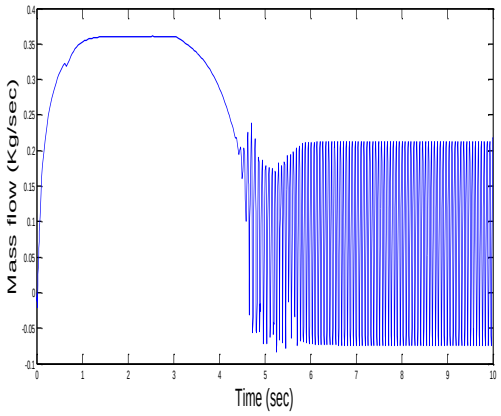

B. Throttle flow

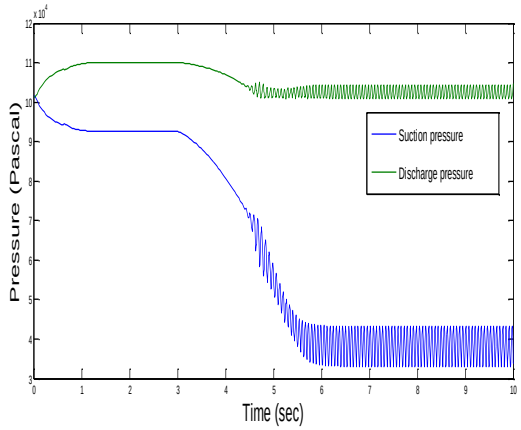

C. Pressures

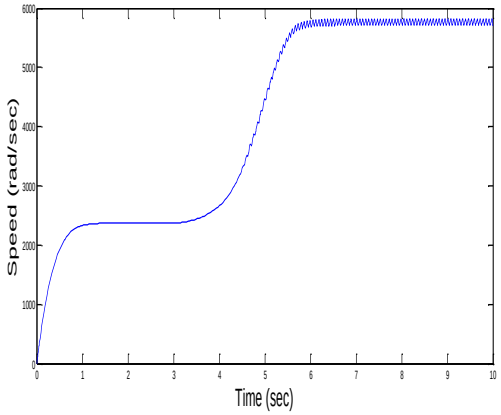

D. Compressor speed

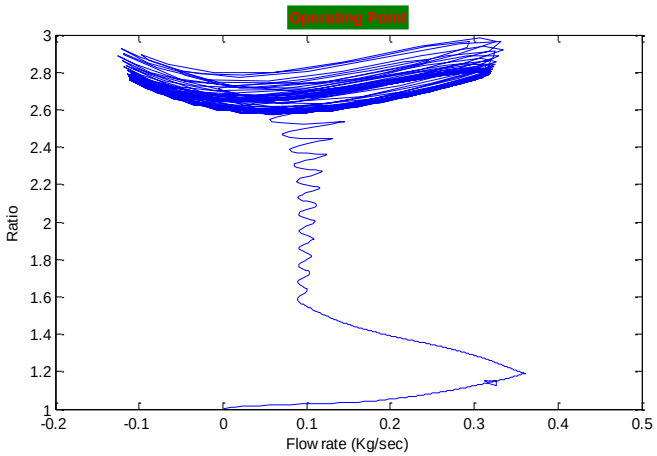

E. Compressor operating point

Figure 2.7: Simulation Results of the Open Loop System

2.3.4. Discussion of the results

The **Figure 2.7** shows the behaviour of a centrifugal compressor described by the modified Greitzer model. We let the throttle valve 100% open. Initially the compressor is stable and the design mass flow rate for the compressor is 0.361 kg/sec. To disturb our system or in other words make it enter the surge region, we had to reduce the feed flow. To do so, we forced the feed flow valve to close starting from t = 3 sec, then the mas flow starts to decrease towards lower mass flow rates. The compressor remains stable until approximately t=4.3sec where the feed flow valve is completely closed. This transition between the stable and the unstable state of the compressor is due to the decrease of the charge on the compressor blades until the operating point reaches the surge point (t=4.3sec). It can be found from the simulation results that the surge cycle has a frequency of approximately 6 Hz. The suction pressure and the discharge pressure decrease; the discharge pressure decreases from 11 x 10^4 Pa to 10.45 x 10^4 Pa then enters to a cyclic behaviour, and the suction pressure decreases from 10.15 x 10^4 Pa to 7 x 10^4 Pa (**Fig.2.7.C**) to enter a cyclic behaviour. Whereas, rotating speed of the compressor and the pressure ratio increase to a higher value. The rotating speed increases from 2400 rad/s to approximately 5800 rad/s. This increase of speed and pressure ratio is due to the small load applied on the impellers. The operating point of the compressor enters surge once the feed valve is completely closed (**Fig.2.7.E**).

2.4. Compressor closed loop modelling (recycle mode)

In the closed loop configuration, a throttle flow is fed back to the compressor via the recycle valve. (Figure below)

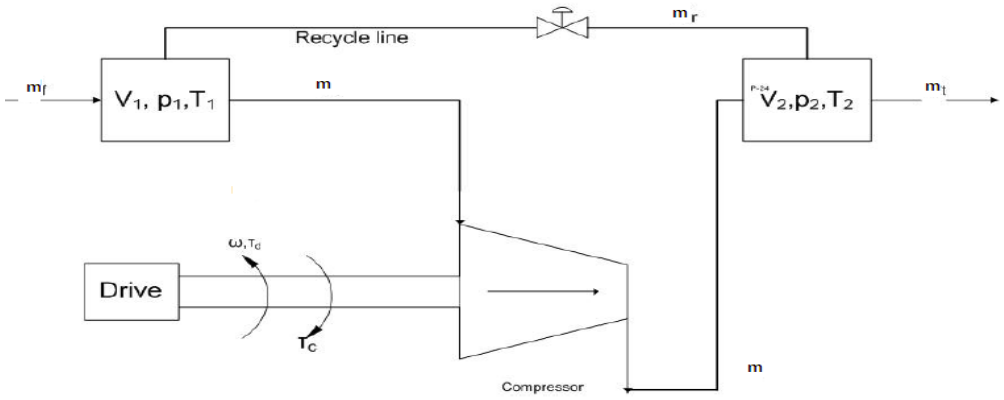

Figure 2.8: A Centrifugal Compressor with Recycle Loop and Motor **[19].**

Applying the mass balance principle to the downstream volume shown in Figure 2.8:

$$V_1\dot{\rho}_1 = m_f - m + m_r \qquad (\mathbf{2.23})$$

Where V_1 is the downstream volume, m_f is mass flow into the downstream volume and m is the mass flow through the compressor. m_r is the recycle mass flow given as :

$$m_r = k_r\sqrt{\Delta p_r} \qquad (\mathbf{2.24})$$

k_r is a gain proportional to the opening of the valve in the recycle loop and Δp_r is the pressure drop across the recycle valve.

Assuming that the gas is ideal and isentropic it can be shown that:

$$\dot{p}_1 = a_{01}^2\dot{\rho}_1 \qquad (\mathbf{2.25})$$

Combining the Eqs 2.23 and Eqs 2.25, the final equation for the mass balance of the downstream volume is: $\dot{p}_1 = \frac{a_{01}^2}{V_1}\left(m_f - m + m_r\right)$ $(\mathbf{2.26})$

We assume the same sonic velocity of the gas in the upstream volume, the mass balance can now here be described by: $\dot{p}_2 = \frac{a_{01}^2}{V_2}(m - m_r - m_t)$ $(\mathbf{2.27})$

The expression for mass flow in the duct from the outlet of the compressor to the upstream volume in **Fig2.8** is developed based on the momentum balance. **[19]**

This expression is defined as follows:

$$\dot{m} = \frac{A_1}{L_c}(\psi_c(m,\omega)p_1 - p_2) \qquad (\mathbf{2.28})$$

The resulting compressor model with a recycle line driven by a shaft can be summarized as:

$$\dot{p}_1 = \frac{a_{01}^2}{V_1}\left(m_f - m + m_r\right)$$

$$\dot{p}_2 = \frac{a_{01}^2}{V_2}(m - m_r - m_t)$$

$$\dot{m} = \frac{A_1}{L_c}(\psi_c(m,\omega)p_1 - p_2)$$

$$\dot{\omega} = \frac{1}{J}(\tau_d - \tau_c) \qquad (\mathbf{2.29})$$

2.4.1. Model simulation and results

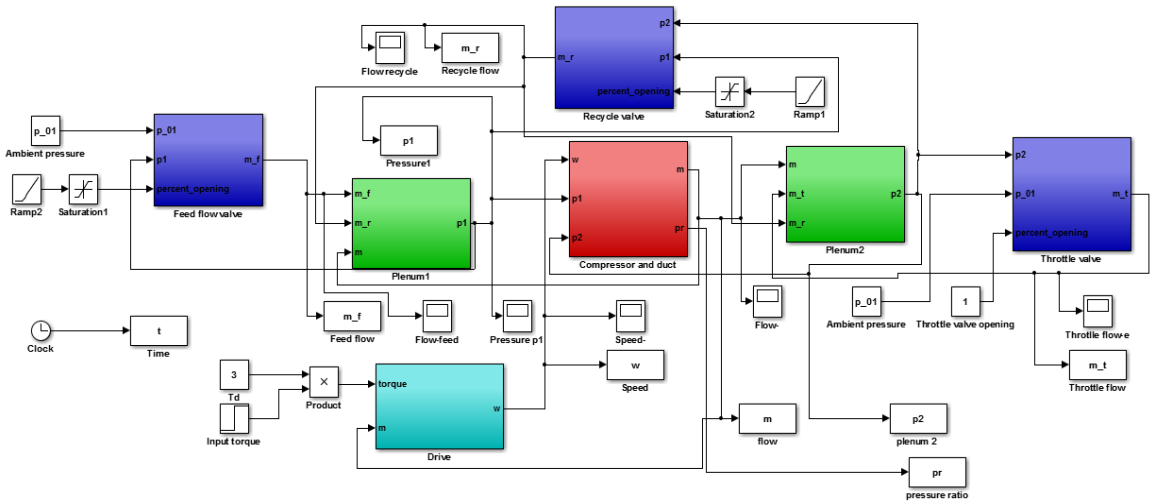

Figure 2.9: Simulink Circuit of the Closed Loop Model

The following graphs are obtained after running the above Simulink file:

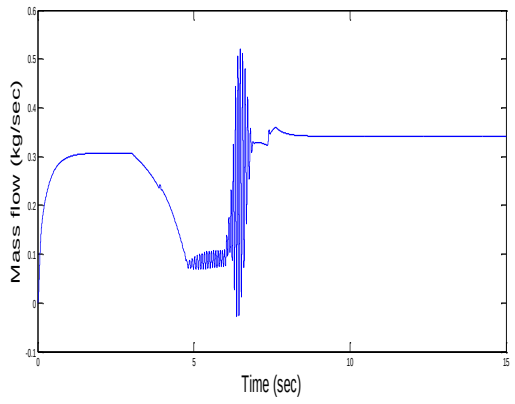

A. Mass flow

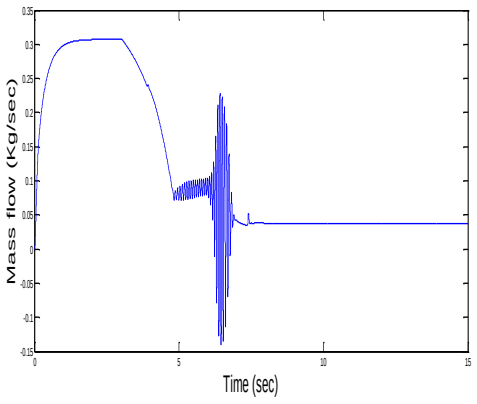

B. Throttle flow

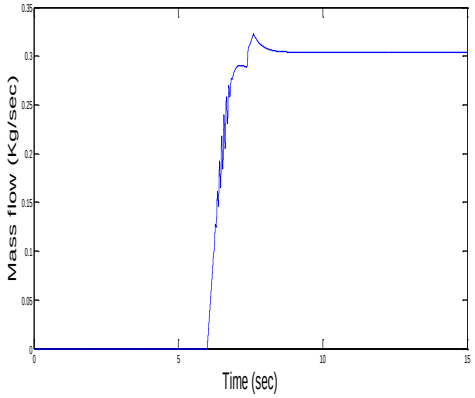

C. Recycle flow

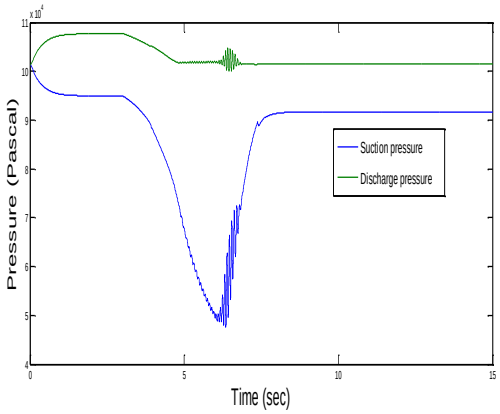

D. Pressures

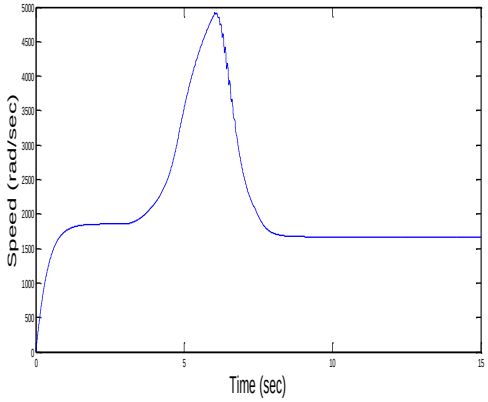

E. Compressor speed

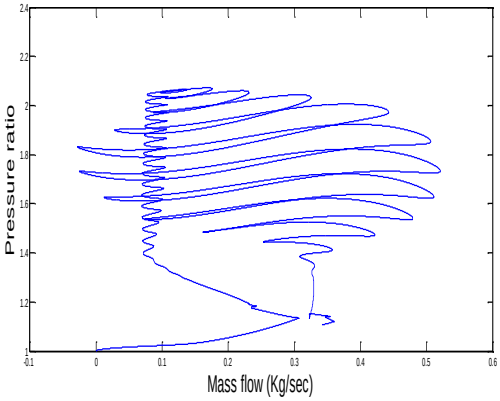

F. Compressor operating point

Figure 2.10: Simulink Results of the Closed Loop

2.4.2. Discussion

The recycle mode is used to eliminate the surge manually. This is done by inserting a recycle valve that feedback the throttle flow to the compressor (plenum 1) and opening it whenever the compressor is likely to enter the surge. The simulation results shown in **Figure 2.10** show the results of opening the recycle valve at time t=6sec on the different parameters of our compressor. Before t=6sec, **Figure 2.10** shows that the obtained simulation results are the same as the ones of open loop mode, that is:

At t=3sec, the feed flow valve begins to close causing the operating point to move towards the surge region, the compressor and throttle flows begin to decrease, the discharge and the suction pressures as well while the speed starts to increase due to the small load applied on the impellers. This remains until t=4.10sec where the compressor enters the surge.

From t=4.10sec to t=6sec:

- Discharge pressure decreases from 11x 10^4 Pa to 10.15 x 10^4 Pa, the suction pressure decreases also from 9.35 x 10^4 Pa to around 4 x 10^4 Pa (**Fig.2.10.D**).
- Rotating speed increases from 2400 rad/s to around 6000rad/s. (**Fig.2.10.E**).

At t=6sec, the manual control of our compressor via the recycle valve starts. Once the valve starts to open, more mass flow through the system is allowed by compensation of the flow in the suction plenum. The higher mass flow leads the operating point to shift to the right and the surge begins to disappear making the compressor stable.

* When the recycle valve is opened:

- The compressor speed decreases due to the higher mass flow load applied on the impellers and stabilizes at 1650rad/s.
- The mass flow stabilizes at 0.35 kg/s.
- The suction and the discharge pressures stabilise at 9.15 x 10^4 Pa and 10.15 x 10^4 Pa respectively.

2.5. Conclusion

In this chapter, a detailed literature of the modelling of compressors has been presented. The models stated include the linear and the nonlinear ones. We used the developed Greitzer nonlinear model to describe the internal dynamics of our compressor in both open loop and closed loop configurations. A simulation using Matlab-Simulink was done to the two model configurations.

From the results of this simulation, we can conclude that when the flow rate is under certain small value, the compressor enters the surge region thereby becomes unstable unless a recycle valve, located between the suction and discharge tanks, is used. It is clearly seen from the simulation results that when the recycle valve is opened, the flow is upheld in the safe region where the compressor behaves stably.

Since the valve should always be opened manually, this latter must be controlled. In the next chapter, a method of controlling the recycle valve is going to be used.

Chapter Three

PID CONTROL OF THE RECYCLE VALVE

3.1. Introduction

When a compressor reaches its surge condition, the entire system becomes unstable. This will cause severe damages to the compression system. Preventing the surge phenomena becomes then an obligation. Various preventing techniques and anti-surge control techniques were developed and used through literature but the most common way is to recycle a portion of the flow and the discharge to keep the compressor away from its surge limit. To do so, a recycle valve is inserted between the discharge plenum and the suction one. Thus, preventing the surge is controlling the percentage opening of this valve; this limits the operation of the compressor to flow rates. The control action consists to open the valve by a certain amount when the operating point of the system approaches a certain line called the surge-control (SCL) defined based on the surge margin for a particular compressor. A PID controller may be very efficient as anti-surge control technique. To confirm that, it will be used in this chapter as a control technique.

3.2. PID controller

Proportional-Integral-Derivative (PID) control is the most common control algorithm used in industry and has been universally accepted in industrial control. The popularity of PID controllers can be attributed partly to their robust performance in a wide range of operating conditions and partly to their functional simplicity, which allows engineers to operate them in a simple, straightforward manner. As the name suggests, PID algorithm consists of three basic coefficients; proportional, integral and derivative which are varied to get optimal response. **[20]**

3.2.1. PID structure

PID controller is a control loop feedback controller according to **Figure 3.1**.

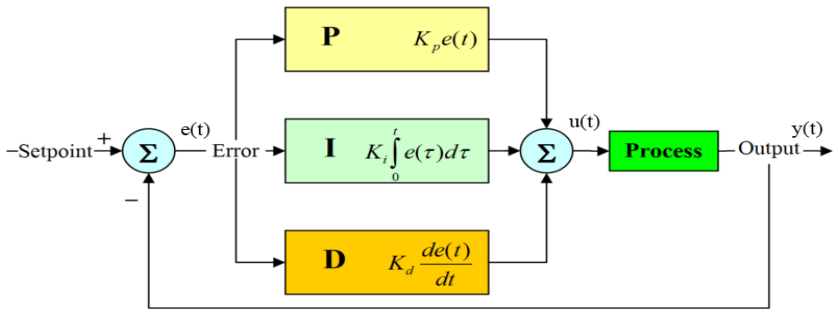

Figure 3.1: A block diagram of a PID controller in a feedback loop. **[21]**

e(t) is the tracking error and y(t) is controlled (output) variable.

- K_p is the proportional gain;
- K_I is the integral time;
- K_d is the derivative time.

The control input is given as:

$$u(t) = Kpe(t) + Ki\int_0^t e(\tau)d\tau + Kd\frac{de(t)}{dt} \quad \textbf{(3.1)}$$

Equivalently, the transfer function in the Laplace Domain of the PID controller is

$$L(s) = Kp + \frac{Ki}{s} + Kd \quad \textbf{(3.2)}$$

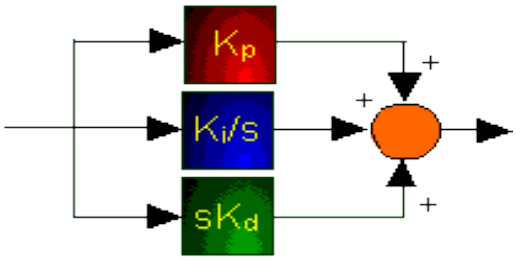

Figure 3.2: PID Controlled System. **[20]**

3.2.2. Effect of a PID Controller parameters on a system characteristics:

The P, I and D parameters of a PID controller affect the system dynamic. Four main characteristics of the closed-loop step response are evaluated:

- **Rising time:** The time it takes for the control system output to rise beyond 90% of the desired level for the first time.
- **Overshoot:** How much the peak level is higher than the steady state, normalized against the steady state.
- **Settling time:** The time it takes for the system to converge to its steady state.
- **Static error:** The difference between the steady-state output and the desired output.

The following figure gives a more clear idea about the four characteristic of a closed loop step response.

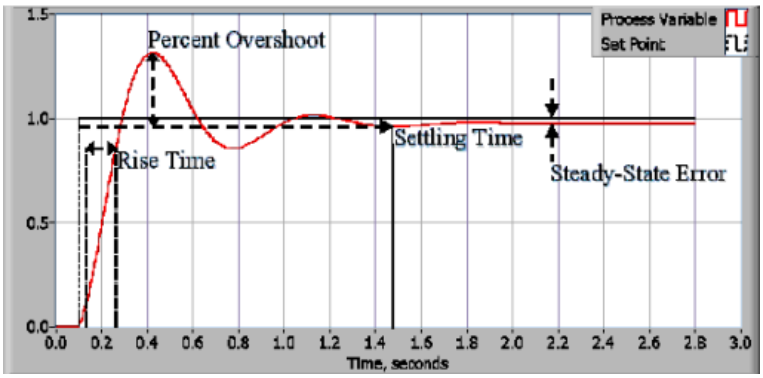

Figure 3.3: Step response of a PID. **[20]**

Proportional term effect: The proportional gain (K_p) determines the ratio of output response to the error signal. In general, increasing the proportional gain will increase the speed of the control system response. However, if the proportional gain is too large, the process variable will begin to oscillate. If K_p is increased further, the oscillations will become larger and the system will become unstable and may even oscillate out of control.

Integral term effect: The integral component sums the error term over time. The result is that even a small error term will cause the integral component to increase slowly. The integral response will continually increase over time unless the error is zero, so the effect is to drive the Steady-State error to zero. Steady-State error is the final difference between the process variable and set point. However, since the integral term responds to accumulated errors from the past, it can cause the present value to overshoot the set-point value.

Derivative term effect: The derivative component causes the output to decrease if the process variable is increasing rapidly. The derivative response is proportional to the rate of change of the process variable. Increasing the derivative time (T_d) parameter will cause the control system to react more strongly to changes in the error term and will increase the speed of the overall control system response. **[20]**

The following table summarises the effects of P, I and D parameters on the system performance.

Parameter	Rise Time	Overshoot	Settling Time	Static Error
P	Decrease	Increase	Small Change	Decrease
I	Decrease	Increase	Increase	Eliminate
D	Small Change	Decrease	Decrease	Small Change

Table 3.1: Effect of increasing the PID parameters independently.

Playing with the values of the three parameters (independently) of a PID as shown above in the table is one method of tuning a PID controller.

Another manual method is the Ziegler–Nichols method (open loop and closed loop) which is a trial and error tuning method based on sustained oscillations that was first proposed by Ziegler and Nichols (1942). This method that is probably the most known and the most widely used method for tuning of PID controllers. K_i and K_d gains are first set to zero. The proportional gain is increased until it reaches the ultimate gain, K_u, at which the output of the loop starts oscillating. K_u and the oscillation period T_u are used to set the gains as shown in the following table. **[22]**

Control Type	K_p	K_i	K_d
P	$0.50K_u$	-	-
PI	$0.45K_u$	$1.2K_p/T_u$	-
PID	$0.60K_u$	$2Kp/T_u$	$K_pT_u/8$

Table 3.2: Ziegler-Nichols method. **[22]**

Most modern industrial facilities no longer tune loops using the manual calculation methods. Instead, PID tuning and loop optimization software are used to ensure consistent results. These software packages will gather the data, develop process models, and suggest optimal tuning.

Mathematical PID loop tuning induces an impulse in the system, and then uses the controlled system's frequency response to design the PID loop values. In loops with response times of several minutes, mathematical loop tuning is recommended, because trial and error can take days just to find a stable set of loop values. Optimal values are harder to find. Some digital loop controllers offer a self-tuning feature in which very small set-point changes are sent to the process, allowing the controller itself to calculate optimal tuning values.

Other formulas are available to tune the loop according to different performance criteria. Many patented formulas are now embedded within PID tuning software and hardware modules. **[23]**

3.3. Control of the recycle compression system using PID controller

Surge in turbo compressor systems is a very fast phenomenon, even too fast to be detected by conventional instruments. Therefore surge must be prevented rather than controlled. These systems, although they prevent surge rather than control surge, are commonly called “surge control systems”.

To control or more conveniently to prevent the surge, generally the opening of the recycle valve, which is considered as an actuator, is controlled using different control techniques or algorithms:

- Standard PID type algorithm;
- Genetic anti-surge controller;
- Intelligent regulator (Fuzzy Logic)
- Advanced controller;
- Predictive controller

In this chapter, we will use the PID controller to prevent the operation of the compressor in the unstable region.

The surge in a compressor occurs when the system is operating at small flow rates. In a compressor map, the surge is described with a surge line (SL) in the compressor map. This line lies points which are near the maximum of different compressor characteristic curves corresponding to different shaft speeds. To avoid any entrance to instability region, a surge control line (SCL) is drawn parallel (in the right) to the SL. Depending on the operating point of the compressor (whether it is, on the left or on the right of the SCL), the PID controller should send a signal to the recycle valve to either open or close.

When the operating point is right to the surge control line, the controller is off. When the operating point is left to the surge control line, a PID-controller is used to bring the operating point back to the right.

3.3.1. Principle of PID controller in Recycle Compression systems

We now define a new constant “d” which represents the horizontal difference distance between the current operating (P_1) point of the compressor and the surge control line (SCL) in the compressor map. (**Figure 3.4**)

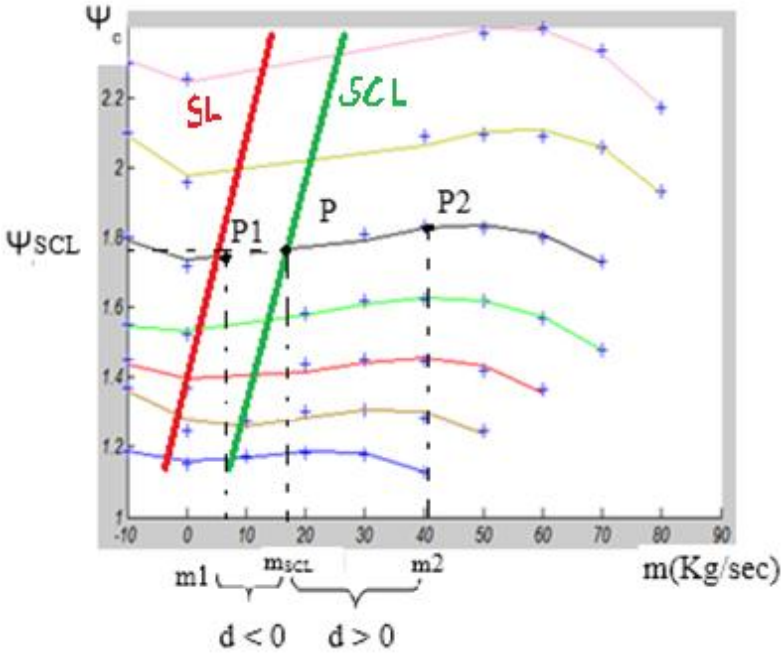

Figure 3.4: Outline of a Recycle Controller.

Where:

$$d = m_i - m_{SCL} \quad \textbf{(3.3)}$$

And $m_i$is the mass flow of the operating point P_i and m_{iSCL} is its corresponding surge control line mass flow.

The SCL is estimated to be linear having the following form:

$$\psi_{SCL} = a * m_{SCL} + b \quad \textbf{(3.4)}$$

Then $$m_{SCL} = \frac{\psi_{SCL} - b}{a} \quad \textbf{(3.5)}$$

Where:

- a: The slope of protection line;
- b: The horizontal surge margin to the surge line;
- ψ_{SCL}: The pressure ratio of the surge control line (SCL) &
- m_{SCL}: The flow of the surge control line (SCL).

Remark

- The coefficients "a" and "b" are approximated from the data given by the s-trim supercharger's manufacturer (using Least Square Estimator).

When the distance "d" is positive, the operating point is located to the right of the control line, then nothing should be done. In other words: the controller must be off.

When the distance is negative, i.e. the operating point is located to left of the control line, in this case, its positive value is used as input to the controller to turn it on.

The error then can be defined as:

$$e = \begin{cases} 0 & d > 0 \\ -d & Otherwise \end{cases} \quad (\mathbf{3.6}) \quad (\mathbf{3.7})$$

Thus, the output of PID controller is given by:

$$v(t) = K_p e(t) + K_i \int e(t) + K_D \frac{de(t)}{dt} \quad (\mathbf{3.8})$$

This output signal controls the percentage opening, or the flow percentage of the recycle valve. So the recycle valve equation will be:

$$m_r = uA_r\sqrt{(p_2 - p_1)} \quad \mathbf{(3.9)}$$

The three parameters used of the PID are found by trial and error method. They are found to be as follows; **P=5**, **I=0.005** and **D=0.15**.

The following Simulink block is constructed to calculate the distance difference "d" then check its sign. If it's negative, the value "–d" will be used as an input reference of the PID controller. This latter computes the signal "u".

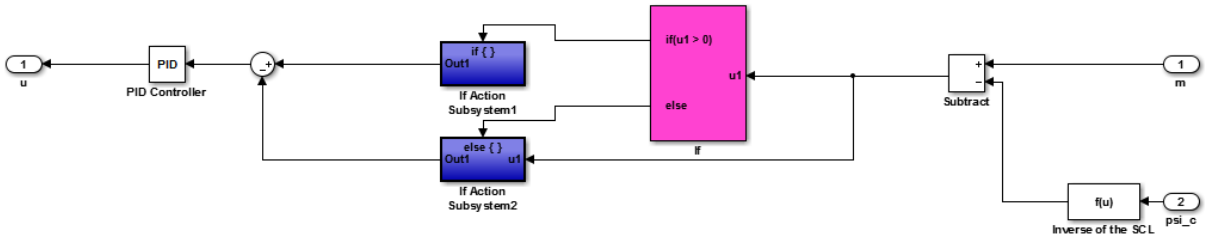

Figure 3.5: Controller structure.

3.4. Simulation and Results:

3.4.1. Simulation results with opening and then closing feed flow valve once:

The following Simulink model describes the whole controlled compression system which contains the sub-block represented in figure 3.5. The results after running are depicted also.

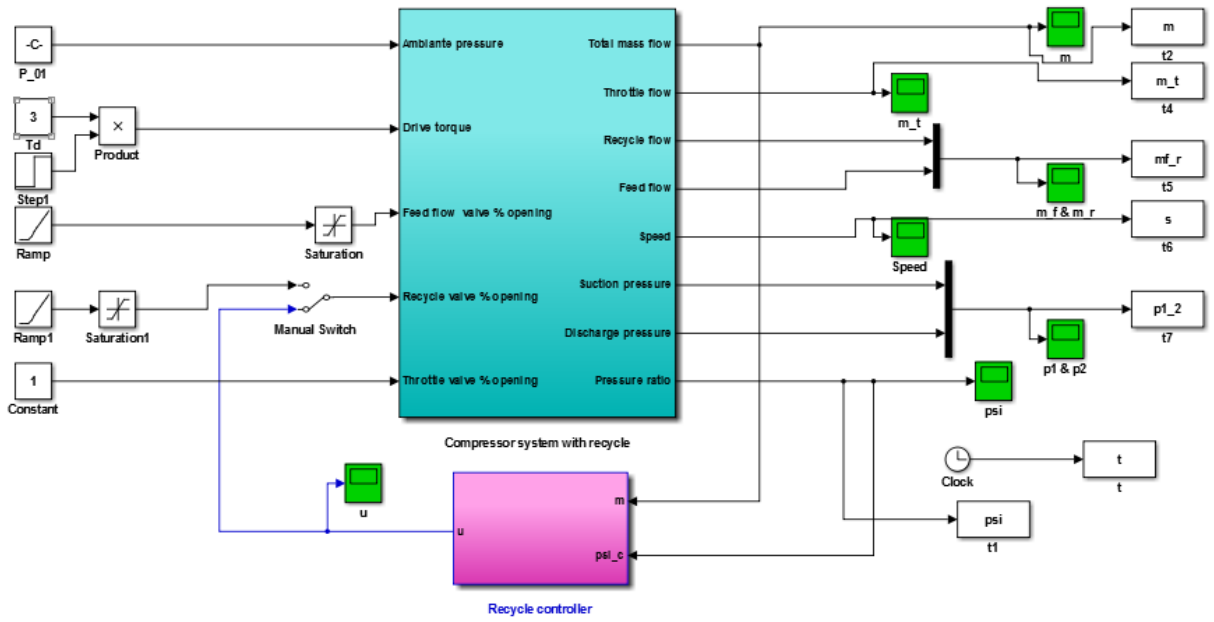

Figure3.6: The Simulated System.

The results after running the Simulink block shown below:

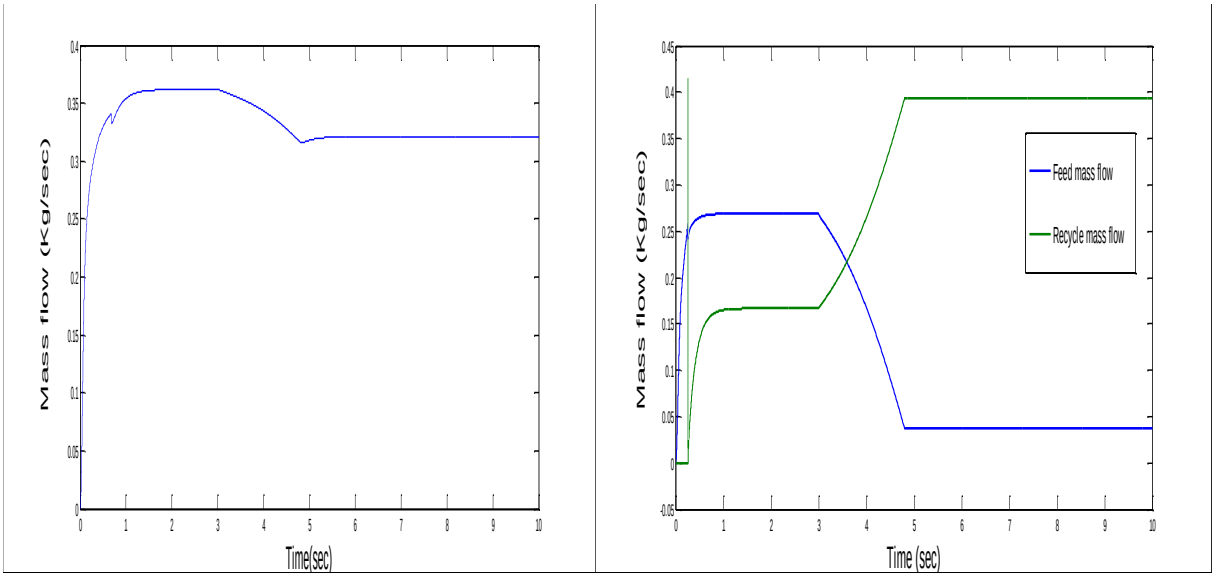

A. Compressor mass flow **B.** Feed and recycle mass flows

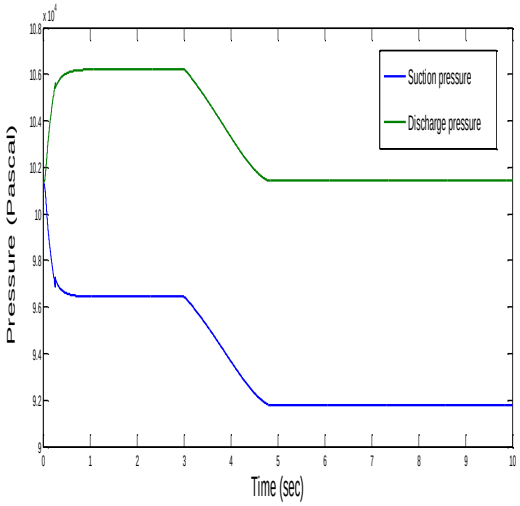

C. Discharge & suction pressures

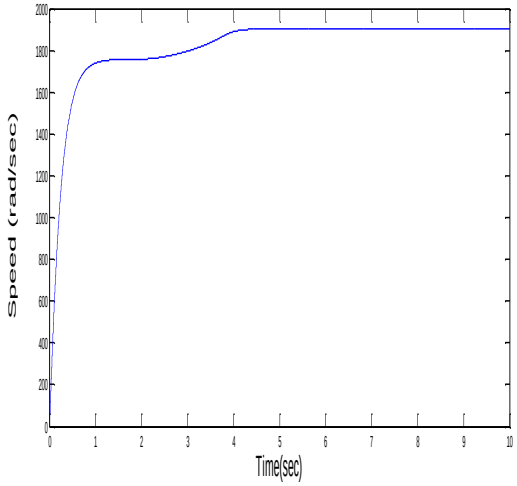

D. Impeller speed

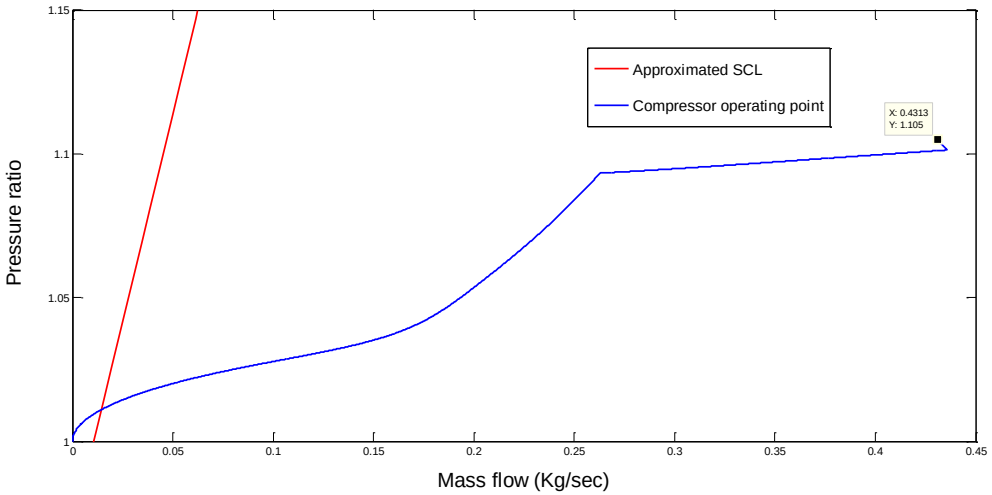

E. Compressor operating point

Figure 3.7: Results of the Simulation.

3.4.1.1. Discussion of the simulation results:

To check whether the tuned PID controller prevents the surge, a perturbation is introduced to the system at time t_1=3sec by closing the feed flow valve gradually. We can see clearly from **figure 3.7.B** that the recycle valve starts to open. This is manifested by the gradual increase of the recycle flow until it stabilises at **0.16kg/sec**. This means that starting from t_1, the tuned PID control is activated opening gradually the recycle valve to compensate the compressor flow at the suction and preventing the operating point form being at the left of the surge control line, thus stabilizing the system; This is can be seen from **figure 3.7.E** where the operating point of the studied compressor is always at the right of the surge control line (in the

stable region) except at the lower flows (so it is better to start the compression system manually) but the controller brings it quickly to the right.

- **Figure 3.7.A** represents the total flow through the compressor where we can see that just after t_1, the flow decreases slightly form **0.47 Kg/s** to **0.43Kg/s** and then increases a bit to **0.44Kg/sec** and stabilizes there.
- The evolution of the speed can be noticed from **Figure 3.7.D** where it's to be noticed that the speed of compressor increases from zero to **1750 rad/sec** before t_1 and once the feed valve closes, the speed increases slightly further to reach and stabilize at **1930 rad/sec**.
- **Figure 3.7.C** represents the discharge and the suction pressures. The discharge decreases when the feed valve starts to close from **$10.8*10^4$ PA** to **$10.14*10^4$ PA** and stabilizes there, whereas the suction decreases from **$09.7*10^4$ Pa** to **$09.15*10^3$ Pa** and remains there also.

3.4.2. Simulation and Results with Alternating Feed Flow Valve:

Changing the position of the manual switch to the alternating signal (sine wave with saturation) will open the feed flow valve then close it for several times periodically, this allows to see how the system is robust and able to reject the disturbances that may happen. The system is represented in the following figure:

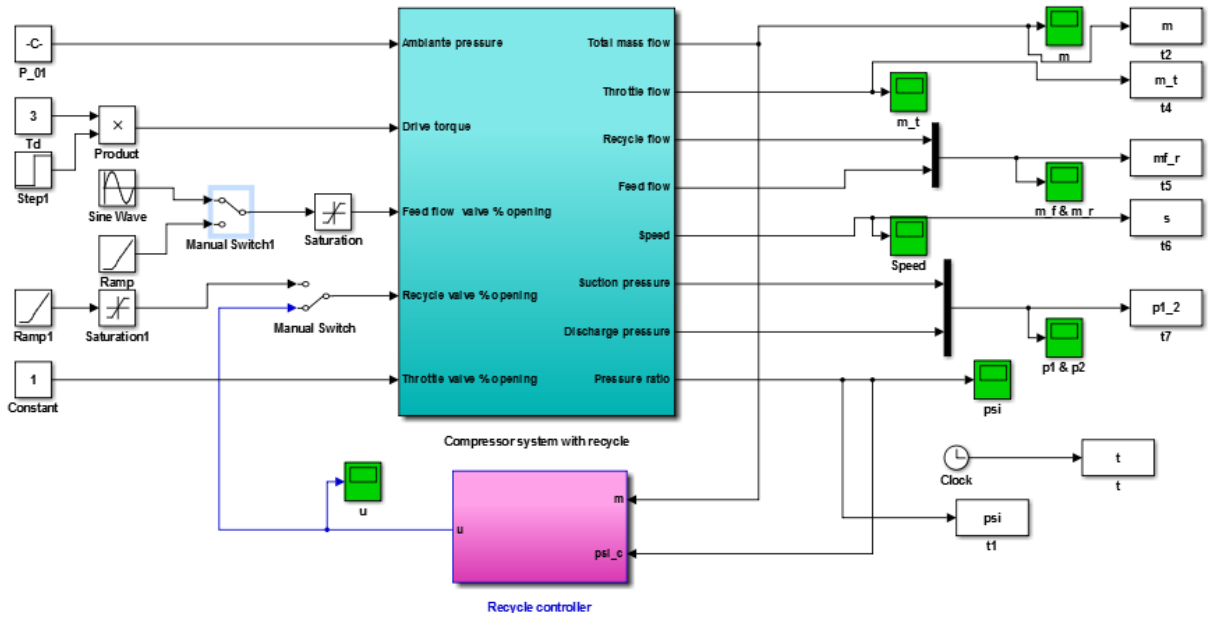

Figure 3.8: The simulated system.

Here are the simulation results after running the above block:

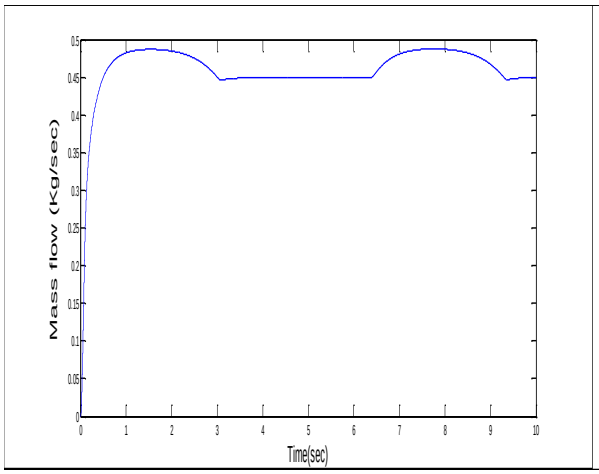

A.Compressor mass flow

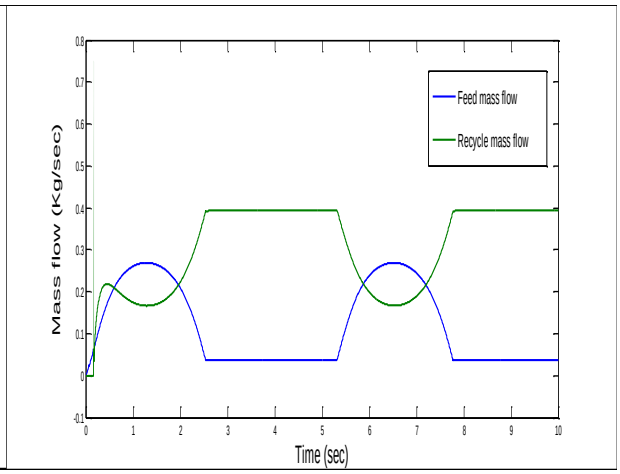

B. Feed and recycle mass flows

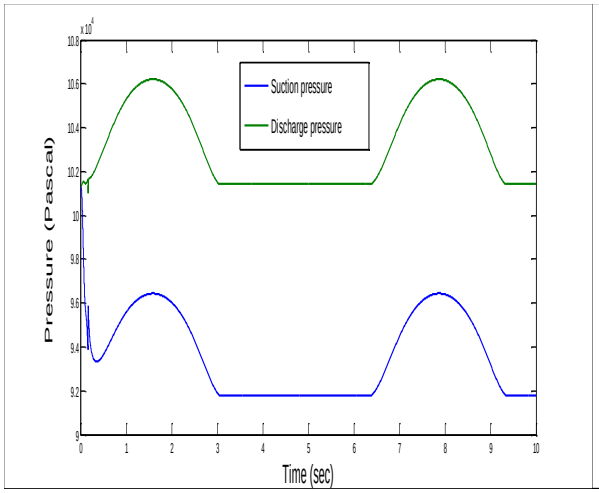

C. Discharge & suction pressures

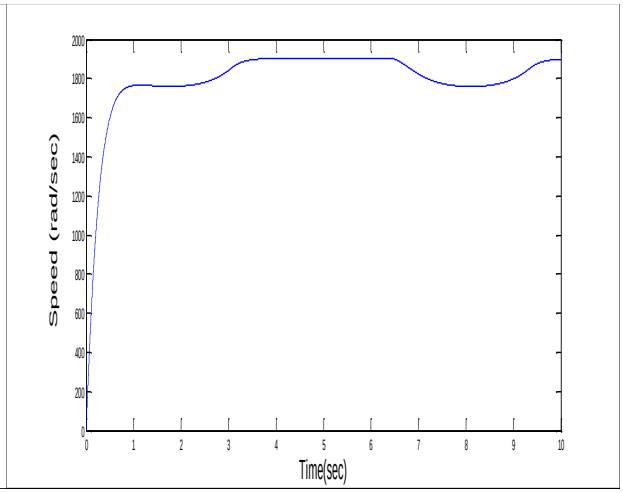

D. Impeller speed

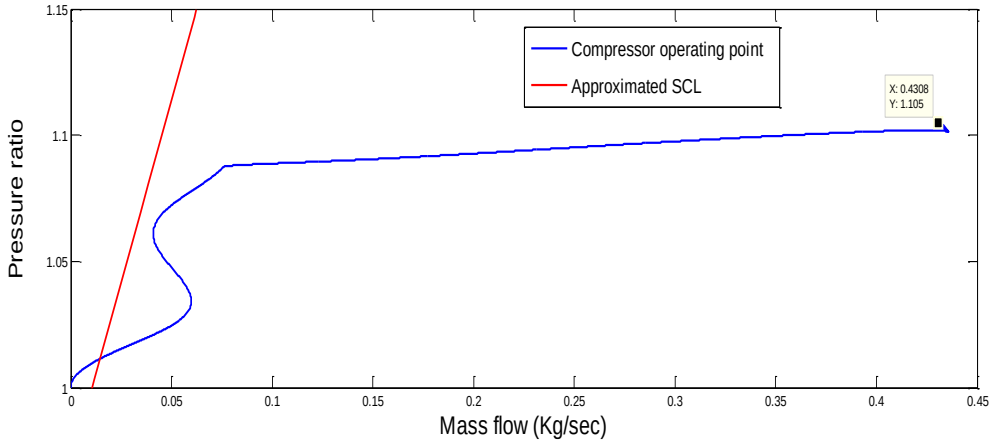

E. Compressor operating point

Figure 3.9: Results of the simulation using periodic input.

3.4.2.1. Discussion of the simulation results

To evaluate the robustness and the ability of the compressor to reject disturbances, a periodic open/close signal is applied to the opening of the feed flow valve.

At **t=2sec** the PID control opens progressively, the recycle valve compensates the compressor flow at the suction preventing the operating point form being in the left of the surge control line.

When the sine signal has a positive slope, the feed flow valve closes gradually leading to the increase of the feed flow. This is logic since there is no need to compensate the compressor flow at the suction.

Since the disturbance signal is periodic, the system is disturbed again but stabilized after by the PID controller.

3.5. Conclusion

In this chapter, a classical PID controller was used to avoid and prevent the surge phenomenon. Before going through the controlling method, a detailed explanation of the PID controller was given. This controller regulates the percent opening of the recycle valve based on information on the current operating point of the compression system; whether it is in the right or in the left of the defined compressor's surge control line.

Based on the obtained figures describing different internal dynamics of the compression system, we can see that the PID did stabilise the system (works in the stable region) and the surge was avoided. The mass flow was stabilised in around (1sec) no overshoot.

An intelligent regulator, applying the technique of the artificial intelligence which is PSO is going to be used in the next chapter. This is done to push the operating point further to the left but never reach the surge line. By doing this, the mass flow should decrease while the pressure ration of the compressor should increase.

Chapter Four

CONTROL OF RECYCLE VALVE USING PSO OPTIMISING ALGORITHM

4.1. Introduction

Metaheuristic algorithms are becoming an important part of modern optimization. A wide range of metaheuristic algorithms has emerged over the last two decades, and many metaheuristics such as particle swarm optimization are becoming increasingly popular.

In this chapter, we will be using the particle swarm optimization (PSO) algorithm to find the maxima of the characteristic curve performance of our compressor which define its surge line. Working just near the maxima point of the performance insures a high efficiency of the compressor.

We are going to write a PSO code that suits our problem, the code will be implemented in Simulink block describing the different dynamics of our compression system. The simulation of this implementation gives specific results and graphs that will be discussed and compared to those obtained when using a PID during the previous chapter.

4.2. Optimisation algorithms

The never ending search for productivity has made optimisation a fundamental concern for engineers. Quick process, low energy consumption, short and economical supply chains are now key success factors. Optimisation problems are concerned with finding the values for one or several decision variables that best meet the objective(s) without violating any constraint. Many of numerical optimisation problems cannot be solved analytically and might even be non-differentiable. Thus, gradient based methods (calculus) cannot be used. Numerical algorithms were then proposed to solve these problems.

Several meta-heuristic methods have been developed to solve various optimisation problems. These can be classified into different groups: deterministic, iterative, stochastic, population-based, etc. An algorithms that works with a set of solution is called as iterative algorithm based on population. **[24].** Depending on the nature of the phenomenon simulated by the algorithms, the population-based heuristic algorithms have two important groups: Evolutionary Algorithms (EA) and swarm intelligence based algorithms. Some of the recognized evolutionary algorithms are: Genetic Algorithms (GA), Differential Evolution (DE), Evolution Strategy (ES), Evolution Programming (EP), Artificial Immune Algorithm (AIA), and Bacteria Foraging Optimisation (BFO) etc. Some of the well-known swarm intelligence based algorithms are: Particle Swarm Optimization (PSO), Ant Colony Optimisation (ACO), Shuffled Frog Leaping (SFL), and Artificial Bee Colony (ABC) algorithms, etc. Besides the evolutionary and swarm intelligence based algorithms, there are some other algorithms which

work on the principles of different natural phenomena. Some of them are: the Harmony Search (HS) algorithm, the Gravitational Search Algorithm (GSA). Biogeography-Based Optimisation (BBO), the Grenade Explosion Method (GEM), the league championship algorithm and the charged system search. **[25]**

Many meta-heuristic algorithms have been devised and modified. Scientists now work on Hybrid global optimization methods to improve the performance of the stated optimising algorithms. They attempt to combine the beneficial features of two or more algorithms to come up with an algorithm that can be powerful for solving challenging non convex optimisation problems. **[26].**

In this chapter, the particle swarm-optimising algorithm is going to be used to find maxima's of the characteristic curves of our compressor for better efficiency.

4.3. Particle Swarm Optimisation (PSO) algorithm for controlling the recycle valve

4.3.1. Introduction and overview

Particle Swarm Optimisation was first introduced by Dr. Russell C. Eberhart and Dr. James Kennedy in 1995. The initial ideas on particle swarms of Kennedy who is a social psychologist and Eberhart who is an electrical engineer were essentially aimed at producing computational intelligence by exploiting simple analogues of social interaction, rather than purely individual cognitive abilities. **[27]**

The PSO algorithm simulates the behaviours of bird flocking. When a group of birds are randomly searching food in an area. There is only one piece of food in the area being searched. All the birds do not know where the food is. But they know how far the food is in each iteration. The best and effective strategy to find the food is to follow the bird that is nearest to the food.

PSO learned from the scenario and used it to solve the optimisation problems. In PSO, each single solution is a "bird" in the search space. It is called "particle". All of particles have fitness values that are evaluated by the fitness function to be optimized, and have velocities that direct the flying of the particles. The particles fly through the problem space by following the current optimum particles until reaching the optimum point (where the food is). **[28]**

4.3.2. PSO algorithm for optimisation

In *PSO* each solution to the problem at hand is called a particle. At each time *t*, each particle, *i*, has a position in the search space.

$x_{t,i} = < x_{t,i1}, x_{t,i2}, \dots, x_{t,id} >$

Where *d* is the dimensionality of the solutions (number of variables of the problem).

A set of particles $\mathbf{S} = \{ x_1^t, x_2^t, \dots, x_m^t \}$ is called a swarm. Particles have an associated velocity value that they use for *flying* (exploring) through the search space. The velocity of particle '*i*' at time *t* is given by:

$$V_{t,i} = < v_{t,i1}, v_{t,i2}, \dots, v_{t,id} >$$

Where: $v_{t,ik}$ is the velocity for dimension *k* of particle *i* at time *t*.

Particles adjust their flight trajectories after each iteration by using the following updating equations:

- $V_{t+1,i,j} = v_{t,i,j} + c_1 * r_1 * (pbest_{i,j} - x_{t,i,j}) + c_2 * r_2 * (gbest_{g,i} - x_{t,i,j})$ **(4.1)**

- $x_{t+1,i,j} = x_{t,i,j} + v_{t+1,i,j}$ **(4.2)**

Where:

$pbest_{i,j}$ is the value in dimension *j* of the best solution found so far by particle *i*; $pbest_i = < pbest_{i,1}, pbest_{i,2}, \dots, pbest_{i,d} >$ is called personal best. Where each element of is personal best at a certain axis which represent a variable.

$gbest_{g,i}$ is the value in dimension *j* of the best particle found so far (best previous position among all the particles in t-th iteration) in the swarm (**S**) .

$gbest_i = < gbest_{i,1}, gbest_{i,2}, \dots, gbest_{i,d} >$ is considered the leader (global best) particle.

It is to be noted that through *pbest* and *gbest*, each particle "*i*" takes into account individual (local) and social (global) information for updating its velocity and position. In that respect, c_1, $c_2 \in \mathrm{R}$ are constants weighting the influence of local and global best solutions, respectively. r_1, $r_2 \sim U[0,1]$ are values that introduce randomness into the search process.

The swarm is randomly or uniformly initialized, considering restrictions on the values that each dimension can take. Next, the "*goodness"* of each particle is evaluated by the fitness function and $gbest$ and $pbest$ are initialized. Or they can be initialized randomly also by giving them the values of the position of each particle of the swarm.

Then, the iterative *PSO* process starts, in each iteration:

i) The velocities and positions of each particle in every dimension are updated according to Equations (4.1) and (4.2);

ii) The *goodness* of each particle is evaluated using the fitness function;

iii) $gbest$ and $pbest$ are updated if needed for each particle.

This process is repeated until either a maximum number of iterations is reached or a minimum fitness value is obtained by a particle in the swarm and an optimal solution is found.

The fitness function is used to evaluate the aptitude (*goodness*) of candidate solutions. The definition of a specific fitness function depends on the problem at hand; in general, it must reflect the proximity of the solutions to the optima. A fitness function *F:* $Y \rightarrow R$, where Y is the space of particles positions, should return a scalar $\boldsymbol{f(x_i)}$ for each particle position $\mathbf{x}_i$, indicating how far particle *i* is from the optimal solution to the problem at hand. **[29]**

Particle swarm optimization (PSO) has experienced many changes since its introduction in 1995. As researchers have learned about the technique, they have derived new versions, developed new applications, and published theoretical studies of the effects of the various parameters and aspects of the algorithm. **[27]**

In 1998 Shi and Eberhart came up with what they called PSO with inertia. To control the velocity, the inertia weight is multiplied by the previous velocity in the standard velocity equation and is linearly decreased throughout the run.

Another PSO implementation called PSO Constriction Coefficient was developed by Clerc in 2000. Using a constriction coefficient results in particle convergence over time. That is the amplitude of the particle's oscillations decreases as it focuses on the local and neighbourhood previous best points. Though the particle converges to a point over time, the constriction coefficient also prevents collapse if the right social conditions are in place. **[30]**

4.3.3. Neighbourhood topologies [31]

The PSO algorithms can be classified into two main types according to the topology of the swarm global PSO and local PSO. In the (standard) global PSO, all the particles are neighbours of each other (fully connected topology). Therefore the position of the global best particle is propagated to the whole swarm and affects the velocity update. Generally speaking, global PSOs usually converge faster and get trapped in local optima more easily.

In local PSO variants, particles are grouped into neighbourhoods according to a certain strategy. In this variant only the neighbour particles of a given particle can influence its velocity update. Consequently, local PSOs converge slower than global PSOs but are less likely to be captured in local minima due to greater population diversity. An overview of the topologies available is depicted in the picture below:

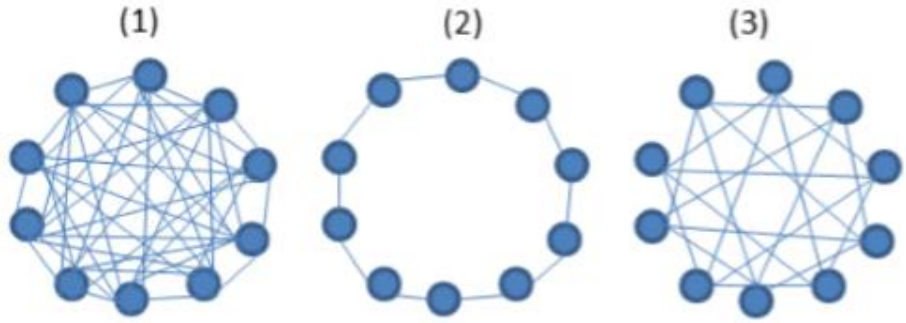

Figure 4.1: Graphical representation (1) Fully connected (2) Ring and (3) Von Neumann topologies.

- **The fully connected topology:** It is the standard configuration where all the particles are neighbours of each other
- **Ring topology:** Every particle is connected with its preceding and its following particle.
- **Von Neumann topology:** Every particle is connected with 4 other particles, the two following and the two previous, wrapping around at the beginning and the end of the population.

4.3.4. Implementation of PSO in Matlab to optimise the Ψ_c function

To write the code of the PSO algorithm that finds the maximums of the Ψ_c function, we used the ring topology where each particle has a local best. The swarm is then divided into sub-swarms of three particles each. The local best of each sub-swarm is obtained by comparing the

fitness value of a particle's personal best with the fitness value of its two neighbours; the preceding one on its right and the following one on its left.

Finally, all the local bests are compared to find their maximum, which is our optimum solution for a specific impeller speed. We also introduced the inertia weight coefficient to Eqs(4.1) to control the increase of the velocity. The following figure shows a flowchart of our PSO algorithm code.

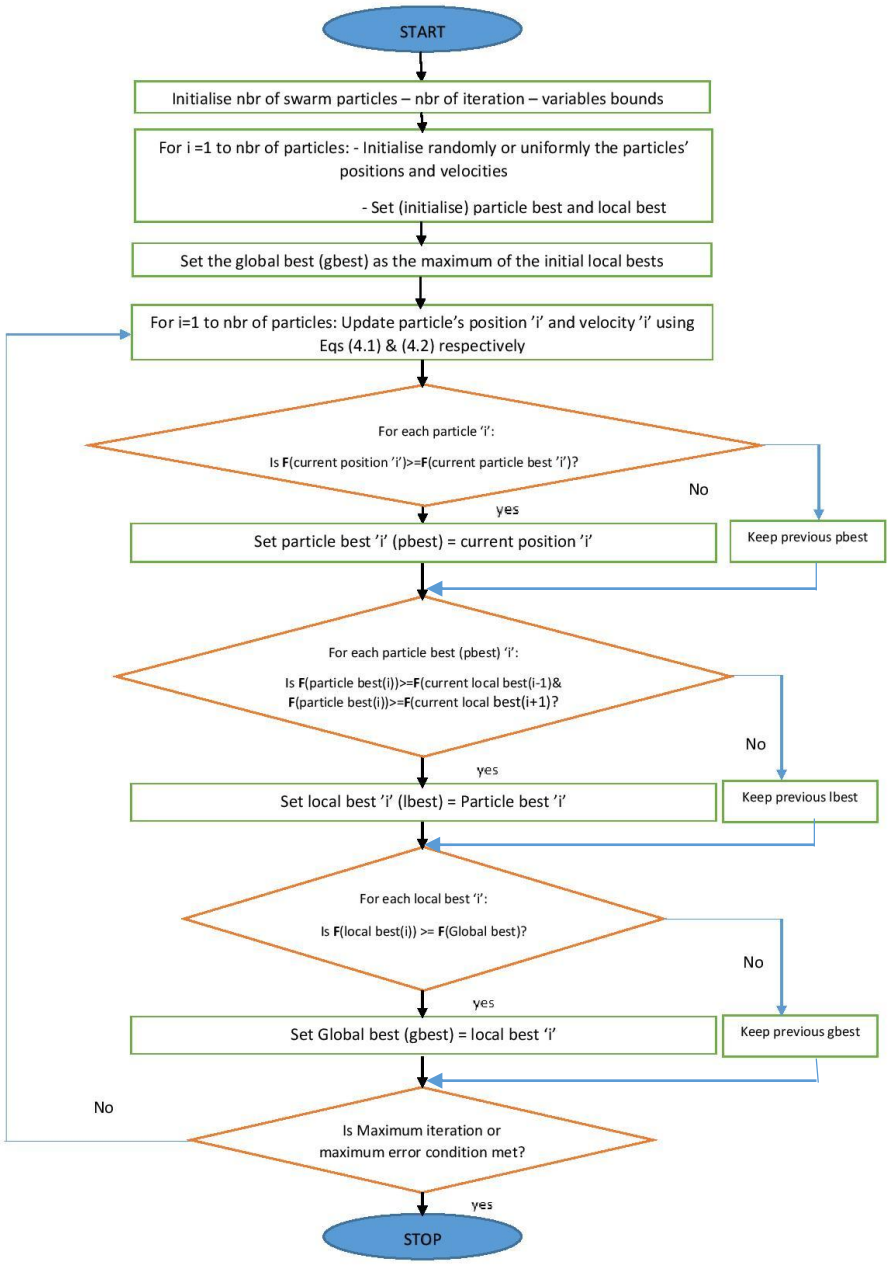

Figure 4.2: Flowchart of the PSO ring-topology algorithm.

The purpose behind the implementation of the PSO algorithm is to find the maximums (for each speed) of the characteristic equation ψ_c of the compressor seen in the second chapter Eqs (2.12), given as:

$$\psi_c(m,\omega) = \left(1 + \frac{\mu r_2^2 \omega^2 - \frac{r_1^2}{2}(\omega - \alpha m)^2 - k_f m^2}{C_p T_{01}} \right)^{\frac{k}{k-1}} \qquad k \neq 1$$

The optimisation is done because it is known that the compressor operates at complete efficiency just near the maxima of its characteristic equation at the limit of the unstable region. These maximum values define the surge line **SL**.

Therefore, our fitness function is be the characteristic equation of the compressor ψ_c. This latter is a function of two variables: the mass flow and the speed.

After substituting the different parameters of the ψ_c equation, this latter will become:

$$\psi_c(\mathrm{m},\omega) = \left(1 + \frac{0.0035 * \omega^2 - 0.00078013(\omega - 9197.9 * m)^2 - 0.0178 * m^2}{20100} \right)^{3.5}$$

To test the written code, let the following speed vector:

$$\omega(rad/sec) = [800\ 850\ 900\ 9501000\ 1050\ 1100\ 1150\ 1200\ 12501300\ 1350\ 1400]$$

We run the written code to obtain the maxima of the fitness function (ψ_c) for every speed of the previous vector. The surge control line **SCL** can also be found by just adding a safe margin to the **SL.**

The points defining the two lines are shown in the following table:

Speed (rad/sec)	m_{SL}(Kg/sec)	ψ_{SL}	m_{SCL}	ψ_{SCL}
800	0.0880	1.4474	0.0968	1.4460
850	0.0920	1.5139	0.1020	1.5128
900	0.0960	1.5868	0.1056	1.5859
950	0.1040	1.6667	0.1140	1.6646
1000	0.1080	1.7538	0.1188	1.7521
1050	0.1160	1.8489	0.12760	1.8457
1100	0.1200	1.9526	0.1320	1.9497
1150	0.1240	2.0665	0.1364	2.0629
1200	0.1320	2.1881	0.1452	2.1838
1250	0.1360	2.3216	0.1496	2.3138
1300	0.1400	2.4665	0.1540	2.4630
1350	0.1480	2.6239	0.1628	2.6180
1400	0.1520	2.7946	0.1672	2.7893

Table 4.1: The extreme values of Ψc function obtained from the PSO code.

Using the maximum values and their corresponding pressure ratio in the table above, the approximated surge and controlled surge lines are easily obtained using the LSE (least square estimator).

The approximated surge line is found to be equal to: $\Psi_{SL} = 20.2964 m_{SL} - 0.4115$ **(4.3)**

While the approximated surge control line is obtained as: $\Psi_{SCL} = 18.3884 m_{SCL} - 0.4062$ **(4.4)**

The Fig.4.2 below shows a resultant compressor map when the compressor is operating at certain speed values with the real surge and surge control lines.

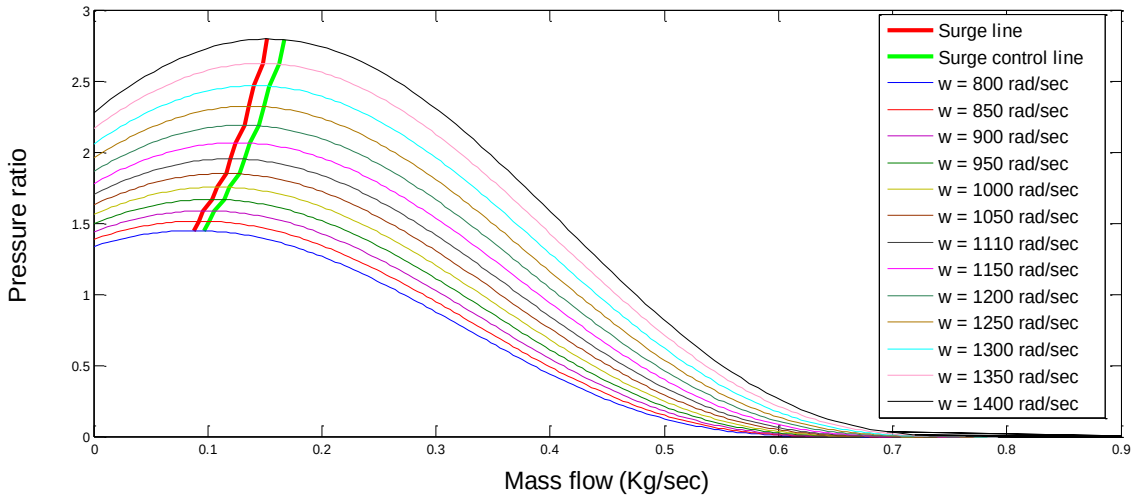

Figure 4.3: Compressor map using PSO algorithm.

4.3.5. Implementation of PSO algorithm in Simulink-Matlab

The written code of PSO Algorithm is used in this part to create a Simulink block that controls our compression system. Again, the main idea of using PSO is to find the maximum values of the ψ_c function defining the surge. A PID controller is also used to control the percentage of opening the recycle valve.

As known, the compressor operates at full pressure ratio or 100% efficiency at maxima of the compressor characteristic (psi function). Therefore, the implemented optimising block calls the PSO code instantaneously to compute the value of the mass flow (m_{SL}) corresponding to those maxima (Ψ_{SL}).

These values of mass flow represent the minimum flow values that allow the compressor to operate in the safe stable region; if the compressor operates at any smaller values, it enters the surge. A safe margin of 10% is added to these (m_{SL}) values to get the m_{SCL} values.

At each instant, each (m_{SCL}) value given by the PSO algorithm is compared with the actual operating mass flow 'm' of the system. Where:

$$\boldsymbol{Diff = m - m_{SCL}} \quad \textbf{(4.5)}$$

Then, if the difference is positive, the tuned PID will be off while if it is negative the tuned controller will be activated.

The error signal which is the input of our PID controller is given as:

$$e = \begin{cases} 0 & d > 0 \\ -d & Otherwise \end{cases} \quad \textbf{(4.6)}$$

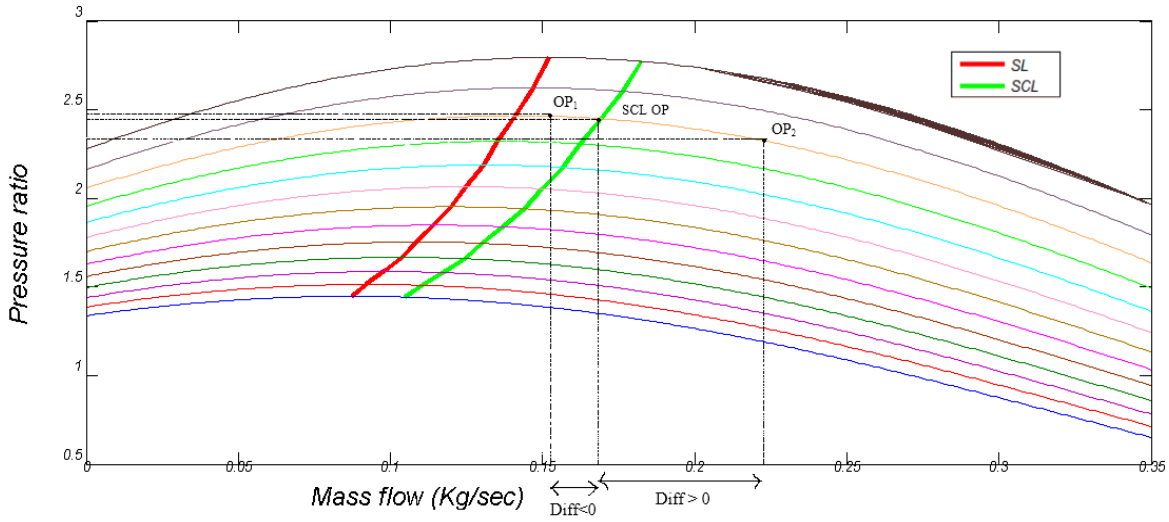

Figure 4.4: The PSO strategy of controlling a recycle valve.

Remarks

- The tuned PID is used to minimise the harmonics that occur during the simulation. The values of its parameters used are as follows: **P=125**, **I=6.5** and **D=8**.
- In this part, we do not approximate the points defining the surge line as an equation of a straight line. Each point is taken apart to get larger pressure ratio.

4.3.6. Simulation results

We expect from the simulation results that the pressure ratio to increase to a greater value than the one obtained using the PID, and the mass flow to decrease, because we want to push the operating point to the left near the points defining the surge but never reach them. As the mass flow would decrease, we expect the speed of the impellers to increase due to the small load applied on the impellers.

The following graphs are the simulation results of the model controlled using PSO:

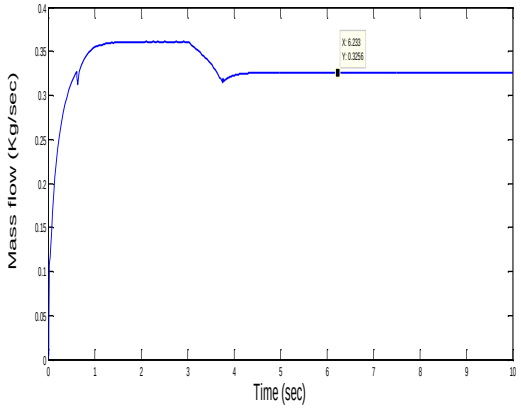

A. Mass flow

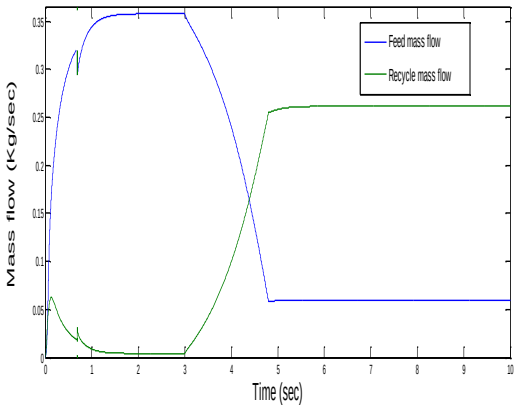

B. Feed and recycle flows

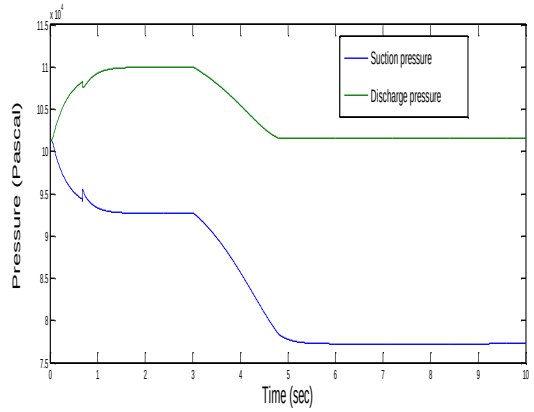

C. Pressures

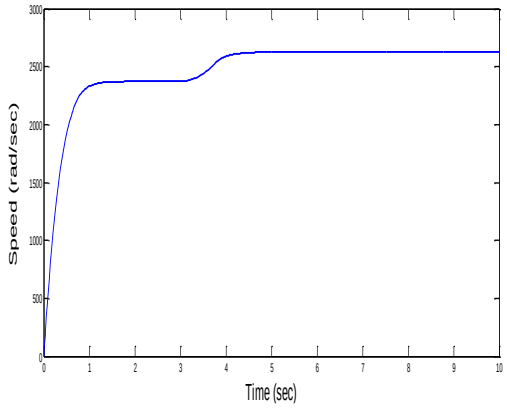

D. compressor speed

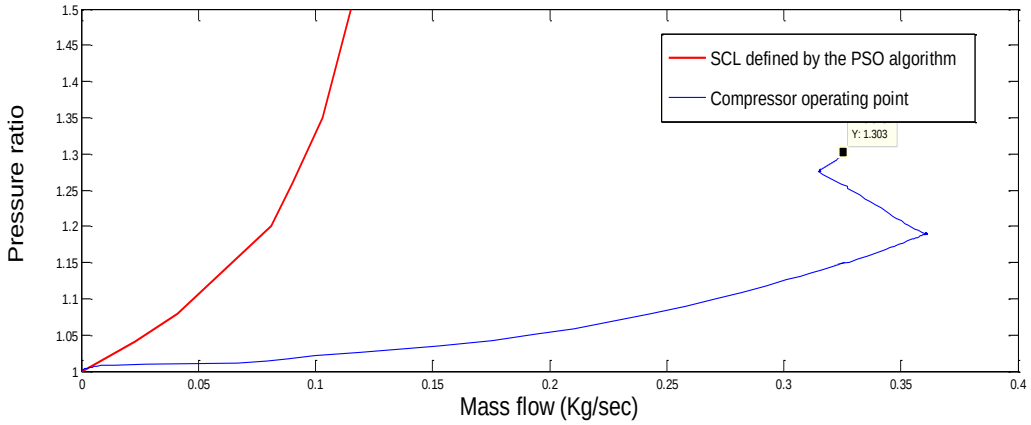

E. Compressor operating point

Figure 4.5: Simulation Results of the controlling using the PSO algorithm.

4.3.7. Discussion

We can see from the simulation results of **Figure 4.5** that the expected results were obtained. This can be seen for example from **Figure 4.5.A,** representing the mass flow; after the feed valve was completely closed, the mass flow stabilises at **0.3256 Kg/sec** which is a value smaller than the stabilised mass flow value of 0.**44 Kg/sec** obtained using just the PID controller. This indicates that the operating point of our compressor was pushed a bit to the left towards the surge control line defined by the PSO algorithm. This can be illustrated by **Figure 4.5.E,** where one can see that the value of the pressure ratio was increased using the PSO algorithm to a value of **1.303,** which was **1.104** using only the PID. The operating point is always to the right of the points defining the surge.

Since the stabilised value of the mass flow decreased comparing with the one of the PID, less load will be applied on the compressor impeller causing the speed to increase. **Figure 4.5.D** confirms this as the speed stabilised at **2640 rad/sec**, which is greater than **2000 rad/sec**, the stabilised value obtained using the PID.

4.4. Conclusion

To increase the efficiency (pressure ratio) of our compressor system and maintain its stability, we applied the particle swarm optimisation (PSO) algorithm along with the PID controller. The PSO is used to find, at each instant, the maxima of the compressor characteristic equation describing the pressure ratio taking into consideration temperature, entropy, flow rate etc. The mass flow value corresponding to each maxima is then compared with the actual mass flow. This difference was fed to the input of the tuned PID controller, which is used to minimise the harmonics that occur during the simulation. Comparing the results of this chapter with the previous one in which the points defining the surge were approximated as a straight-line equation, the pressure ratio did increase from **1.104** when using the approximated surge line and the PID to **1.303** when the PSO was introduced with the PID. The stabilised total mass flow value decreased in this chapter i.e. lesser flow was recycled via the recycle valve meaning surge region was less likely to be entered or reached.

The addition of the PSO algorithm to control the opening of the recycle valve gave great results that match at a high extent our expectations.

Conclusion

Conclusion

Through this thesis, we have firstly treated the **mathematical model** describing the operation of the centrifugal compression systems in its open loop configuration which, in presence of disturbances, the system is driven to its unstable behaviour (surge). In our case, the disturbance was to **close** the feed valve. To overcome this instability, the system is converted into a closed loop one, by introducing a **recycle valve** (this change the previous model) that feedback the output (throttle) flow to the compressor's input plenum, the valve is opened whenever the compressor is likely to enter the surge.

To begin with, a manual opening of the recycle valve is proposed but due to its **high time response**, the compressor enters surge for a period of time then gets stabilised. This can lead to severe **damages** in the centrifugal compressor causing it to work **inefficiently**, and in countries that have an economy all based on hydrocarbon resources like ours, this method of controlling might affect the economic production.

The ineffectiveness of the previous stabilising method and its need to **human resources** monitoring the compression system and intervening in case of an eventual instability, obliged us to **automate** the opening of the recycle valve by introducing a **PID** controller to the closed loop configuration of our system. With a good tuning of the PID, system simulation showed better results; whenever a disturbance is simulated, its effect can successfully be handled by the system, preventing surge. Certain dynamics' behaviour (mass flow, pressures…) decreased after the disturbance, however, the controller quickly raises and smooth them.

In both previous controlling techniques, the instability was prevented at an extent and the system functioned properly. Yet, it has been noticed that the compressor did not worked with high efficiency i.e. the pressure ratio value was not that high. To increase it, the **Particle swarm optimisation (PSO)** algorithms is used. Introducing it to the compressor system **did increase** its pressure ratio and stabilised the different compressors' parameters with along the **PID**.

The stabilisation of the different compressor's dynamics and the optimisation of its pressure ratio were accomplished at the end of this work. As a future work, self-tuning controllers can be used along with other metaheuristic optimising algorithms (GA, Ant colony …) to stabilise the compressor and increase its efficiency.

References

References

1. Jan Tommy Gravdahla, Olav Egelanda & Svein Ove Vatlandb, "*Drive torque actuation in active surge control of centrifugal compressors*", Norwegian University of Science and Technology, June 2002.
2. Department of energy, mines and resources, *"Energy Management series for industry commerce and institutions (Compressor and turbines)".* Ottawa, Canada
3. Johan Liedman & Robert Månsson "*Dynamic simulation of a centrifugal compressor system*", Master of Science Thesis, Department of Chemical and Biological Engineering CHALMERS UNIVERSITY OF TECHNOLOGY Gothenburg, Sweden, 2013.
4. Corina H.J. Meuleman "*Measurement and Unsteady Flow modelling of centrifugal compressor* surge", Technische Universiteit. Eindhoven, 2002.
5. Salim Hamed Thunaiyan Al-Mawali, Jie Zhang *"A FUZZY APPROACH TO ACTIVE SURGE CONTROL OF CENTRIFUGAL COMPRESSORS",* School of Chemical Engineering and Advanced Materials, University of Newcastle upon Tyne.
6. Shepard, Dennis G. "*Principles of Turbo-machinery*", McMillan (1956).
7. A.L Ling-Viska Mulyandasari "*Compressor selection and sizing (Engineering Design Guidelines-Compressors)",* KLM Technology Group. Malaysia, 2008-201.
8. Data H. Ali Marefat, M. R. Shahhosseini, and M. A. Ashjari *"Adapted Design of Process Multi-Stage Centrifugal Compressor and Comparison with Available Data"*
9. Franciscus P.T. Willems *"Modelling and Bounded Feedback Stabilization of Centrifugal Compressor Surge",* Technische Universiteit Eindhoven, 2000. Proefschrift.
10. Greitzer, E.M., *"Surge and rotating stall in axial flow compressors*", ASME J. Eng. Power, Vol. 98. No. 2, April 1967
11. Klečákova *, "Variable composition gas centrifugal compressor anti-surge protection*". 1947, Praha, Czech Republic.
12. VKI Lecture Series 1992. *"Active control of stall and surge".* I.J Day, Whittle laboratory, Cambridge, England.
13. NEVRLÝ, Josef, MAREK, Jiří, VARGOVČÍK, Luboš & OLDŘICH, Jiří *"Centrifugal Compressor Dynamics and Software System or Surge Control",* The 20th International Conference on Hydraulics and Pneumatics, Prague, September 29 – October 1, 2008
14. J. Van Helvoirt "*Centrifugal Compressor Surge Modelling and Identification for Control"*, Technische Universiteit. Eindhoven, 2007.
15. A. Cortinovis, D. Pareschi, M. Mercangoez, T. Besselmann, *"Model Predictive Anti-Surge Control of Centrifugal Compressors with Variable-Speed Drives*", University of Science and Technology, Trondheim, Norway , May 31 - June 1, 2012

REFERENCES

16. Jan Tommy Gravdahl & Olav Egeland "*Centrifugal Compressor Surge and Speed Control", IEEE.* May 2003.

17. Jan Tommy Gravdahl, Olav Egeland "*Centrifugal Compressor Surge and Speed Control", IEEE.* September 1999.

18. Jan Tommy Gravdahl, Olav Egeland and Svein OveVatland "*Drive torque actuation in active surge control of centrifugal compressors"*, Dept. of Engineering Cybernetics Norwegian U. of Science and Tech. January 2002.

19. Tove Helene Hovd "*Modelling, state observation and control of Compression System"*, Department of Engineering Cybernetics, Norwegian University of Science and Technology. May 2007.

20. PID Theory Explained. http://www.ni.com/white-paper/3782/en/

21. PID controller. https://en.wikipedia.org/wiki/PID_controller#cite_note-21

22. Mohammad Shahrokhi and Alireza Zomorrodi "*PID Controller Tuning Methods*", Sharif University of Technology Comparison.

23. Y Li, KH Ang, GCY Chong, "*Patents software and hardware for PID control: An overview and analysis of the current art Control Systems"* IEEE, 26 (1), 42-54.

24. Patricia Mellin Oscar Castillo Janusz Kasprzyk, *"Design of intelligent systems based on fuzzy logic, neural networks and nature-inspired optimisation".*

25. R. Venkata Rao, Vivek Patel, *"An improved teaching-learning-based optimisation algorithm for solving unconstrained optimization problems",* Department of Mechanical Engineering, S.V. National Institute of Technology, Ichchanath, Surat, Gujarat – 395007 , India, October 9, 2012.

26. J. L. Klepeis, M. J. Pieja, and C. A. Floudas, *"Hybrid Global Optimization Algorithms for Protein Structure Prediction: Alternating Hybrids"*, February, *2003.*

27. Riccardo Poli · James Kennedy · Tim Blackwell, *"Particle swarm optimization"* Received: 19 December 2006 / Accepted: 10 May 2007.

28. PSO Tutorial. http://www.swarmintelligence.org/tutorials.php

29. Hugo Jair Escalante Manuel Montes Luis Enrique Sucar, *"Particle Swarm Model Selection Journal of Machine Learning Research 10 (2009) 405-440"* - Department of Computational Sciences National Institute of Astrophysics, Optics and Electronics Puebla, Mexico, 72840.

30. Matthew Settles, *"An Introduction to Particle Swarm Optimization"* lecture. Department of Computer Science, University of Idaho, Moscow, Idaho U.S.A 83844 November 7, 2005.

31. Particle Swarm Optimisation. http://dev.heuristiclab.com/trac.fcgi/wiki/Documentation/Reference/Particle%20Swarm%20Optimization

32. Bjørn Ove Barstad, *"The Compressor Recycle System"* Norwegian university of science and technology, August 2010.

Appendices

Appendix A [18]

The compression process is modelled as an isentropic compression from p_{01} to p_{02} followed by an isobaric entropy increase. The change in stagnation enthalpy in the isentropic compression is denoted Δh_{0s}, while according to Ferguson (1963) the entropy increase is due to the shock loss Δh_{0i} related to incidence loss at the blade inlet and in the diffuser, and the fluid friction loss Δh_{0f}. The total increase $\Delta h0t$ of the stagnation enthalpy of the fluid contributed by the rotor is

$$\Delta h_{0t}(\omega,m) = \Delta h0s(\omega,m) + \Delta h0i(\omega,m) + \Delta h0f\ (m) \qquad \textbf{(A.1)}$$

The compressor characteristic is defined by:

$$\psi_c(m,\omega) = \frac{P_{02}}{P_{01}}, \qquad \textbf{(A.2)}$$

Then, from the standard isentropic relations we get:

$$\psi_c(m,\omega) = \left(\frac{T_{ocs}}{T_{01}}\right)^{\frac{k}{k-1}} = \left(1 + \frac{\Delta h_{0s}}{C_p T_{01}}\right)^{\frac{k}{k-1}} \qquad \textbf{(A.3)}$$

Where T0cs is the stagnation temperature that would result at the rotor outlet if the compression from p01 to Ψcp01 had been isentropic, and

$\Delta h_{0s}(\omega,m) = \Delta h_{0t}(\omega,m) - \Delta h_{0i}(\omega,m) - \Delta h_{0f}\ (m)$ **(A.4)**

Following Ferguson (1963), we assume the following expressions for the changes in stagnation enthalpy:

$\Delta h_{0t} = \mu r2^2\omega^2$ (A.5a)

$\Delta h_{0i} = r^2/2(\omega - \alpha m)^2$ (A.5b)

$\Delta h_{0f} = k_f m^2$ (A.5c)

It is emphasized that the controller design and stability analysis presented below will still be valid for more elaborate expressions for the changes in stagnation enthalpy. In fact, the results that are presented are also valid for numerical approximations of the compressor characteristic φ_c (ω,m).

Combining the (A.3), (A.4) and (A.5), the following expression is found for the compressor characteristic:

$$\psi_c(m,\omega) = \left(1 + \frac{\mu r_2^2\omega^2 - \frac{r_1^2}{2}(\omega-\alpha m)^2 - k_f m^2}{C_p T_{01}}\right)^{\frac{k}{k-1}} \qquad \text{With} \quad k\neq 1 \qquad \textbf{(A.6)}$$

Appendix B [32]

```
%% COMPRESSOR CHARACTERISTIC APPROXIMATION
%%
%% Compressor type: Vortech S-trim


%% AUTHOR: Bjørn Ove Barstad

% CALCULATION OF ZERO FLOW PRESSURE RATIO
%kappa = c_p / c_v, air
kappa = 1.4;
%sonic velocity
c_plenum = 343;
%ambient temperature 30 deg C
T_01 = 303.15;
%inducer diameter
D1 = 0.079;
%impeller perimeter diameter
D2 = 0.119;

%speedvector
N = [20000 25000 30000 35000 40000 45000 50000]; %RPM (speed)

%zero flow pressure ratio
%eq. 13.50 in Gravdahl & Egeland 2002
PSI_czero = [];
for i = 1 : length(N)
    PSI_czero = [PSI_czero (1 + (pi^2* (N(i)/60)^2 *(D2^2 - D1^2))/(2*c_plenum*T_01))^(kappa/(kappa - 1))];

end

% MANUAL INSERTION OF POINTS
% FOR DIFFERENT SPEEDLINES
x_corrected = {};
y = {};
```

```
%points for the speedline 20000 rpm
x_corrected(1) = {[-10 0 10 20 30 40]};
y(1) = {[1.19 PSI_czero(1) 1.175 1.185 1.18 1.13]};

%points for the speedline 25000 rpm
x_corrected(2) = {[-10 0 10 20 30 40 50]};
y(2) = {[1.37 PSI_czero(2) 1.275 1.30 1.305 1.285 1.245]};

%points for the speedline 30000 rpm
x_corrected(3) = {[-10 0 20 30 40 50 60]};
y(3) = {[1.45 PSI_czero(3) 1.435 1.45 1.445 1.42 1.365]};

%points for the speedline 35000 rpm
x_corrected(4) = {[-10 0 20 30 40 50 60 70]};
y(4) = {[1.55 PSI_czero(4) 1.58 1.617 1.625 1.617 1.57 1.48]};

%points for the speedline 40000 rpm
x_corrected(5) = {[-10 0 30 40 50 60 70]};
y(5) = {[1.80 PSI_czero(5) 1.81 1.83 1.825 1.8 1.733]};

%points for the speedline 45000 rpm
x_corrected(6) = {[-10 0 40 50 60 70 80]};
y(6) = {[2.10 PSI_czero(6) 2.09 2.095 2.09 2.06 1.93]};

%points for the speedline 50000 rpm
x_corrected(7) = {[-10 0 50 60 70 80]};
y(7) = {[2.30 PSI_czero(7) 2.385 2.4 2.335 2.17]};

X_CORRECTED = [];
Y = [];
for i = 1 : length(x_corrected)
    for j = 1 : length(x_corrected{i})
        X_CORRECTED = [X_CORRECTED x_corrected{i}(j)];
        Y = [Y y{i}(j)];
    end
end
```

```
hold on
scrsz = get(0,'ScreenSize');
figure(1);
set(1,'Position',[(scrsz(3)/2 - 466/2) (scrsz(4)/2 - 411/2) 466 411]);
plot(X_CORRECTED, Y,'+'),grid,axis([-10 90 1.0 2.4])
xlabel('Corrected mass flow lb/min')
ylabel('Pressure ratio')

% THIRD ORDER POLYNOMIAL APPROXIMATION
% OF THE SPEEDLINES
%the speedlines will then be continuous
%in mass flow

POLY = [];
for i = 1 : length(x_corrected)
    POLY = [POLY; polyfit(x_corrected{i},y{i},3)];
end
% POLYNOMIAL APPROXIMATION OF THE COEFFICIENTS
%the approximation will then be continuous
%in rotational speed
c = [];
for i = 1 : 4
    c = [c; polyfit(N,[POLY(1,i) POLY(2,i) POLY(3,i) POLY(4,i) POLY(5,i) POLY(6,i) POLY(7,i)],3)];
end
dlmwrite('c_matrix', c);
clear all
```

Figure B.1: Spline approximation of measured data of an S-trim superchargers compressor.